crystals

MDPI

Review

Crystal Chemistry and Structural Complexity of the Uranyl Molybdate Minerals and Synthetic Compounds

Ivan V. Kuporev, **Sophia A. Kalashnikova** and **Vladislav V. Gurzhiy** *

Crystallography Department, Institute of Earth Sciences, St. Petersburg State University, University Emb. 7/9, St. Petersburg 199034, Russia; st054910@student.spbu.ru (I.V.K.); kalashnikova.soff@gmail.com (S.A.K.)
* Correspondence: vladislav.gurzhiy@spbu.ru or vladgeo17@mail.ru

Abstract: This paper reviews not the largest, but at the same time quite an interesting, group of natural and synthetic uranyl molybdate compounds. Nowadays, nine minerals of U and Mo are known, but the crystal structures have only been reported for five of them. Almost an order of magnitude more (69) synthetic compounds are known. A significant discrepancy in the topological types for natural and synthetic phases is shown, which is most likely due to elevated temperatures of laboratory experiments (up to 1000 °C), while natural phases apparently grow at significantly lower temperatures. At the same time, the prevalence of dense topologies (with edge-sharing interpolyhedral linkage) among natural phases can be noted, which is fully consistent with other recently considered mineral groups. Uranyl molybdates demonstrate several similarities with compounds of other U-bearing groups; however, even topological matches do not lead to the appearance of completely isotypic compounds. Structural complexity calculations confirm, in general, crystal chemical observations. Considering the prevalence of dense structures in which coordination polyhedra of uranium and molybdenum are connected through common edges as well as framework architectures, one can expect a less significant influence of interlayer species on the formation of the crystal structure than the main U-bearing complexes. The more structural complexity of the uranyl molybdate units, the more complex of the entire crystal structure is. In addition, there is a tendency for complexity to increase with increasing density of the complex; the simplest structures are vertex-shared, while the complexity increases with the appearance of common edges.

Keywords: uranyl; molybdate; mineral; crystal structure; topology; structural complexity

check for updates

Citation: Kuporev, I.V.; Kalashnikova, S.A.; Gurzhiy, V.V. Crystal Chemistry and Structural Complexity of the Uranyl Molybdate Minerals and Synthetic Compounds. *Crystals* **2024**, *14*, 15. https://doi.org/10.3390/cryst14010015

Academic Editor: Carlos Rodriguez-Navarro

Received: 25 November 2023
Revised: 14 December 2023
Accepted: 20 December 2023
Published: 23 December 2023

1. Introduction

Molybdate compounds are of significant interest due to their importance for industry. They are essential for the production of optics [1], as framework structures of molybdates containing trivalent and rare-earth ions can be attractive phosphor host materials [2]. Molybdates can be used in producing oxide ion and proton conductors [3] and they are also of great interest due to their low or even negative thermal expansion properties [4]. Moreover, molybdenum presents in different oxidation states in compounds, which causes variable coordination environments for this ion [5]. Therefore, a large number of structural types and topologies are possible, and uranyl molybdate compounds are not an exception.

Uranyl molybdates are important constituents of the oxidized zones of molybdenum, polymetallic, and uranium deposits [6]. They may also be important phases in geological repositories for nuclear waste because Mo is one of the fission products generated during burnup of nuclear fuel in a reactor [7].

Uranyl molybdate phases have been discovered during studies of the corrosion products formed as a result of simulation of the conditions in the nuclear waste repository at Yucca Mountain, Nevada. Through the discovery of the phase $(Cs_{2x}Ba_{1-x})[(UO_2)_5(MoO_6)(OH)_6](H_2O)_n$ ($x \approx 0.4$, $n \approx 6$), the possibility of the formation of uranyl molybdates as the result of spent nuclear fuel alteration was confirmed [8]. Moreover, a number of studies have shown that alteration phases may limit the aqueous transport of radionuclides or diffusion of components of spent nuclear fuel [8,9]. Thus, a detailed understanding of the crystal chemistry of these phases is essential for any further material science tasks, including prediction of their impact on the rate of release of radionuclides under repository conditions.

Herein we review the state of art in a family of natural and synthetic uranyl molybdate compounds. The widest structural diversity, which is characteristic of uranium compounds in general, has not spared the group of molybdates. The work provides a review of all currently known uranyl-molybdate minerals and discusses the features of synthetic experiments in connection with the crystal chemical characteristics of the resulting compounds. Calculations of structural complexity parameters complement the general understanding of the U-bearing structural complexes stability and principles of structural architecture formation.

2. Materials and Methods

2.1. Structural Data

For the current review, all structural data deposited in the Inorganic Crystal Structure Database (ICSD; version 5.1.0; release February 2023) and the Cambridge Structural Database (CCDC; WebCSD version; October 2023) were selected and supplemented by the data reported in the most recent publications. Chemical formulae, mineral names, and the crystallographic parameters for all uranyl molybdates of natural and synthetic origin are listed in Tables 1 and 2. In addition, Table 1 contains information on the proposed symmetry and unit cell parameters for the uranyl molybdate minerals with yet undefined crystal structures listed in the IMA Database of Mineral Properties [10].

2.2. Graphical Representation and Anion Topologies

The crystal structures of uranyl molybdate compounds of natural and synthetic origin discussed in this paper are based on the finite clusters, chains, layers, and framework architectures built by the linkage of U- and Mo-centered coordination polyhedra. Uranium(VI) atoms make two short $U^{6+} \equiv O^{2-}$ bonds to form approximately linear UO_2^{2+} uranyl cations (Ur), which are surrounded in the equatorial plane by other four or five O atoms; this results in the formation of a tetra- or pentagonal bipyramids as coordination polyhedra of U(VI) atoms. Molybdenum(VI) atoms are coordinated by four, five, or six O atoms to form tetrahedral, tetragonal pyramidal, or distorted octahedral coordination geometry. The two latter types are closely related. For instance, tetragonal pyramidal (or five-fold) coordination can be obtained if one of the apical ligands in the octahedron moves some distance away (c.a. 2.5 Å) from the central Mo atom.

The topology of the uranyl molybdate substructural complex can be described by two approaches depending on the interpolyhedral linkage between U- and Mo-centered coordination polyhedra. The anion topology approach suggested by Burns et al. [11,12] is used for the description of the uranyl molybdate crystal structures that are based on layers with edge-sharing linkage. The theory of nodal representation, which was suggested by Hawthorne [13] and then successfully improved and implemented by Krivovichev [14,15], is used to describe layers and frameworks with vertex-sharing linkage, as well as 0D and 1D complexes. This approach consists of comparing black and white nodes to Ur and Mo-centered polyhedra, respectively, so that a single or double line between the nodes corresponds to a vertex- or edge-sharing method of polyhedra polymerization.

The black-and-white graph has the following index ccD–U:Mo–#, where *cc* corresponds to the cation-centered type of the interpolyhedral linkage, D indicates dimensionality (0—finite clusters, 1—chains, 2—sheets, and 3—framework), U:Mo ratio, and #—registration number of the unit. The anion topology of the U-bearing sheets has the ring symbol, $p_1^{r1}p_2^{r2}\ldots$, where p is the number of vertices in a topological cycle and r is the number of particular cycle in the reduced fragment of the uranyl molybdate layer.

2.3. Complexity Calculations

Structural complexity calculation is an approach for numerical characterization of various substructural complexes (U-bearing complex, interstitial cations, hydration state, etc.) and their contribution to the organization and to the influence on the structural architecture formation of the crystalline compound in terms of their information content. The current method was developed a decade ago by Krivovichev [16–20], and has been successfully applied in a number of recent works (e.g., [21–29]). It is based on the Shannon information content calculations of per atom (I_G) and per unit cell ($I_{G,total}$) using the following equations:

$$I_G = -\sum\nolimits_{i=1}^{k} p_i \log_2 \ p_i \quad \text{(bits/atom)} \tag{1}$$

$$I_{G,total} = -v \ I_G = -v\sum\nolimits_{i=1}^{k} p_i \ \log_2 \ p_i \ \ \text{(bits/cell)} \tag{2}$$

where k is the number of different crystallographic orbits (independent sites) in the structure and p_i is the random choice probability for an atom from the i-th crystallographic orbit, that is:

$$p_i = m_i/v \tag{3}$$

The reliable comparison of structural complexity values is implementable only for compounds with the same or very close chemical composition (e.g., polymorphs), whereas even insignificant changes (for instance, in a nature of interstitial complexes, hydration state, etc.) could significantly affect the overall complexity parameters. Complexity parameters can be calculated using the ToposPro package [30].

Table 1. Crystallographic characteristics and structural complexity parameters of natural uranyl molybdates.

No.	Chemical Formula	Mineral Name	Sp. Gr.	*a*, Å/ α, °	*b*, Å/ β, °	c, Å/ γ, °	Structural Complexity Parameters, Bits per Atom/Bits per Unit Cell		Ref.
			Infinite Chains				**U-Bearing Unit**	**Entire Structure**	
	cc1–1:2–1								
1	$Cu_4(UO_2)(Mo_2O_8)(OH)_6$	Deloryite	*C*2/*m*	19.940(10)/90	6.116(2)/104.18(5)	5.520(3)/90	2.470/32.106	3.586/125.525	[31–33]
	Layers								
	Sheets of clusters of uranyl polyhedra								
	Uranophane topology, $5^1 4^1 3^1$								
2	$[(UO_2)(MoO_4)(H_2O)](H_2O)$	Umohoite	*P*-1	6.3748(4)/82.64(1)	7.5287(5)/85.95(1)	14.628(1)/89.91(1)	4.000/128.000	4.585/220.078	[34–38]
2a	$(UO_2)[(MoO_4)(H_2O)](H_2O)_{1.45}$	Umohoite	*P*-1	14.69(3)/90.07	7.535(4)/85.9	6.372(3)/97.1	4.000/128.000	4.700/244.423	[39]
2b	$[(UO_2)(MoO_4)(H_2O)](H_2O)$	Umohoite 14A	*P*2$_1$/*c*	6.32/90	7.5/94	57.8/90	5.358/878.639	5.512/992.534	[40]
	Iriginite topology, $5^1 4^3 3^1$								
3	$[(UO_2)(Mo_2O_7)(H_2O)](H_2O)$	Iriginite	*Pbcm*	6.705(1)/90	12.731(2)/90	11.524(2)/90	2.918/140.078	3.741/344.168	[41–44]
	Sheets formed by chains of uranyl polyhedra								
	$5^3 4^3 3^2$								
4	$Ba_{0.5}[(UO_2)_3O_8Mo_2(OH)_3](H_2O)_{\sim 3}$	Baumoite	Monoclinic *	9.8337(3)/90	15.0436(5)/108.978(3)	14.2055(6)/90			[45]
	Sheets of uranyl polyhedra								
	$5^6 4^1 3^8$								
5	$Ca(UO_2)_6(MoO_4OH)_2O_2(OH)_{49}H_2O$	Tengchongite	*C*222$_1$	13.0866(8)/90	17.6794(12)/90	15.6800(9)/90	4.170/200.235	5.387/894.257	[46,47]
	Undefined structures								
6	$H_4U^{4+}(UO_2)_3(MoO_4)_7(H_2O)_{18}$	Moluranite							[42,48]
7	$(UO_2)(Mo^{6+})_5O_{16}(H_2O)_5$	Mourite	C2, *Cm* or C2/*m*	24.426(6)/90	7.185(1)/102.10(1)	9.895(1)/90			[49,50]
8	$Ca[(UO_2)_3(MoO_4)_2(OH)_4](H_2O)_{\sim 5.0}$	Calcurmolite	Monoclinic	16.30(3)/90	25.49(5)/90.07	19.50(6)/90			[51–54]
9	$MgU^{4+}{}_2(MoO_4)_2(OH)_6 \cdot 2H_2O$ (?)	Cousinite							[55,56]
10	$U^{4+}(MoO_4)_2$	Sedovite	Orthorombic	3.36(6)/90	11.08(3)/90	6.42(5)/90			[57]

* modulated structure that was solved in superspace group *X*2/*m*(*a*0*g*)0*s* with *X* = (0, ½, 0, ½).

Table 2. Crystallographic characteristics and structural complexity parameters of synthetic uranyl molybdates.

No.	**Chemical Formula**	**Sp. Gr.**	***a*, Å/ α, °**	***b*, Å/ β, °**	**c, Å/ γ, °**	**Syn. ***	**Structural Complexity Parameters, Bits per Atom/Bits per Unit Cell**		**Ref.**
FINITE CLUSTERS									
	cc0–1:4–1								
11	$Cs_6[(UO_2)(MoO_4)_4]$	*P*-1	11.613(3)/102.713(6)	12.545(3)/95.281(6)	14.466(3)/106.182(6)	SS[850]	5.123/353.488	5.454/474.536	[58]
12	$Rb_6[(UO_2)(MoO_4)_4]$	*C*2/*c*	17.312(1)/90	11.5285(8)/127.634(1)	13.916(1)/90	SS[700]	3.567/164.084	3.961/229.763	[59]
	cc0–1:4–2								
13	$Na_6[(UO_2)(MoO_4)_4]$	*P*-1	7.0958(8)/73.692(2)	9.566(1)/86.621(2)	13.415(2)/82.940(2)	SS[850]	4.524/208.084	4.858/281.763	[7]
14	$Na_3Tl_3[(UO_2)(MoO_4)_4]$	*Pbcn*	20.5823(14)/90	7.4391(5)/90	26.2514(17)/90	HTwA[120]	4.524/832.335	4.858/1127.052	[60]
INFINITE CHAINS									
	cc1–1:1–4								
15	$Cs_2[(UO_2)O(MoO_4)]$	*Pca*2$_1$	12.018(2)/90	12.438(2)/90	17.917(3)/90	SS[870]	4.755/513.528	5.044/665.860	[61]
	cc1–1:2–1								
16	$Cu_4[(UO_2)(MoO_4)_2](OH)_6$	*B*2/*m*	19.8392(11)/90	5.5108(3)/90	6.1009(4)/104.477(4)	HT[280]	2.470/32.106	3.617/104.881	[31]
17	$Li_2[(UO_2)(MoO_4)_2]$	*P*-1	5.3455(4)/108.267(2)	5.8297(4)/100.566(2)	8.2652(6)/104.121(2)	SS[650]	2.777/36.106	2.974/44.603	[62]
	cc1–1:2–10								
18	$Na_6[(UO_2)O(MoO_4)_4]$	*P*-1	7.637(2)/72.329(5)	8.164(2)/79.364(5)	8.746(2)/65.795(4)	SS[850]	3.792/102.382	4.075/134.465	[7]
19	$K_6[(UO_2)_2O(MoO_4)_4]$	*P*-1	7.8282(8)/83.893(2)	7.8298(8)/73.131(2)	10.302(1)/80.338(2)	SS[850]	3.792/102.382	4.075/134.465	[7]
20	$Rb_6[(UO_2)_2O(MoO_4)_4]$	*P*-1	10.1567(5)/76.921(1)	10.1816(5)/76.553(1)	13.1129(6)/65.243(1)	SS[700]	4.755/256.764	5.044/332.930	[58]
	cc1–1:2–16								
21	$Cs_6[(UO_2)_2(MoO_4)_3(MoO_5)]$	*P*-1	10.4275(14)/70.717(2)	15.075(2)/80.382(2)	17.806(2)/86.386(2)	SS[950]	5.755/621.528	6.044/797.860	[63]
	cc1–1:3–2								
22	$Na_3Tl_5[(UO_2)(MoO_4)_3]_2(H_2O)_3$	*P*2$_1$2$_1$2$_1$	10.7662(6)/90	11.9621(6)/90	12.8995(7)/90	HTwA[180]	4.248/322.842	4.700/488.846	[59]
23	$Na_{12.9}Tl_{3.1}[(UO2)(MoO_4)_3]_4(H_2O)_{6.6}$	*P*2/*c*	19.7942(11)/90	7.1913(4)/97.828(1)	22.8835(13)/90	HTwA[120]	5.248/797.685	5.716/1177.419	[59]
	cc1–1:3–3								
24	$K_2[(UO_2)(MoO_4)(IO_3)_2]$	*P*2$_1$/*c*	11.3717(6)/90	7.2903(4)/108.167(1)	15.7122(8)/90	HT[180]	3.459/152.215	4.170/300.235	[64]

Table 2. *Cont.*

No.	Chemical Formula	Sp. Gr.	*a*, Å/ α, °	*b*, Å/ β, °	c, Å/ γ, °	Syn. *	Structural Complexity Parameters, Bits per Atom/Bits per Unit Cell		Ref.
				LAYERS					
				Vertex-sharing interpolyhedral linkage					
	cc2–1:2–4								
25	$Cs_2[(UO_2)(MoO_4)_2]$	$Pbca$	11.762(2)/90	14.081(2)/90	14.323(2)/90	SS[600]	3.700/384.846	3.907/468.827	[65]
26	$Cs_2[(UO_2)(MoO_4)_2](H_2O)$	$P2_1/c$	8.2222(9)/90	11.0993(10)/95.155(8)	13.9992(13)/90	HT[120]	3.700/192.423	4.322/345.754	[65]
27	$Cs_2(UO_2)(MoO_4)_2(H_2O)$	$P2_1/a$	14.031(1)/90	8.272(2)/90	11.067(2)/95.63	HTwA	3.700/192.423	4.322/345.754	[66]
28	$K_2[(UO_2)(MoO_4)_2]$	$P2_1/c$	12.269(5)/90	13.468(5)/95.08(3)	12.857(6)/90	HTwA	4.700/488.846	4.907/588.827	[67]
29	$K_2[(UO_2)(MoO_4)_2](H_2O)$	$P2_1/c$	7.893(2)/90	10.907(2)/98.70(3)	13.558(3)/90	HT[150]	3.700/192.423	4.17/300.235	[68]
30	$Rb_2[(UO_2)(MoO_4)_2]$	$P2_1/c$	12.302(1)/90	13.638(1)/94.975(1)	13.508(1)/90	SS[700]	4.700/488.846	4.907/588.827	[58]
31	$(C_2H_{10}N_2)[(UO_2)(MoO_4)_2]$	P-1	8.4004(4)/86.112(1)	11.2600(5)/86.434(1)	13.1239(6)/76.544(1)	HT[180]	4.700/244.423	5.755/621.528	[69]
32	$Rb_2[(UO_2)(MoO_4)_2](H_2O)$	$P2_1/c$	7.967(3)/90	10.956(4)/96.69(3)	13.679(5)/90	Aq/HT[120–180]	3.700/192.423	4.17/300.235	[70]
33	$Tl_2[(UO_2)(MoO_4)_2]$	$Pca2_1$	10.977(3)/90	14.004(3)/90	14.041(3)/90	SS[600]	4.700/488.846	4.907/588.827	[71]
34	$(C_5H_{14}N_2)[(UO_2)(MoO_4)_2](H_2O)$	$Pbca$	12.697(1)/90	13.247(1)/90	17.793(1)/90	HT[180]	3.700/384.846	5.129/1436.199	[72]
35	$Na_2[(UO_2)(MoO_4)_2](H_2O)_4$	$P2_1/n$	8.9023(5)/90	11.5149(6)/107.743(1)	13.8151(7)/90	HT[120]	3.700/192.423	4.755/513.528	[59]
	cc2–1:2–5								
36	$(C_4H_{12}N_2)[(UO_2)(MoO_4)_2]$	P-1	7.096(1)/97.008(3)	8.388(1)/96.454(2)	11.634(1)/110.456(3)	HT[180]	3.700/96.211	4.954/307.160	[72]
	cc2–1:2–17								
37	$Na_2[(UO_2)(MoO_4)_2]$	$P2_12_12_1$	7.2298(5)/90	11.3240(8)/90	12.0134(8)/90	SS[850]	3.700/192.423	3.907/234.413	[68]
	cc2–2:3–14								
38	Beta-$Cs_2[(UO_2)_2(MoO_4)_3]$	$P4_2/n$	10.1367(8)/90	10.1367(8)/90	16.2831(17)/90	SS[850]	3.488/292.955	3.697/340.168	[73]
	cc2–3:5–1								
39	$[C_3H_9NH^+]_4[(UO_2)_3(MoO_4)_5]$	Cc	16.768(6)/90	20.553(8)/108.195(7)	11.897(4)/90	HT[220]	5.087/345.947	6.492/1168.534	[74]
40	$(NH_3(CH_2)_3NH_3)(H_3O)_2[(UO_2)_3(MoO_4)_5]$	$Pbnm$	10.465(1)/90	16.395(1)/90	20.241(1)/90	HT[180]	4.264/579.895	4.898/1038.319	[72]
	cc2–5:8–1								
41	$(C_6H_{14}N_2)_3[(UO_2)_5(MoO_4)_8](H_2O)_4$	P-1	11.8557(9)/96.734(2)	11.8702(9)/91.107(2)	12.6746(9)/110.193(2)	HT[180]	4.800/263.975	6.041/791.378	[69]

Table 2. *Cont.*

No.	Chemical Formula	Sp. Gr.	*a*, Å/ α, °	*b*, Å/ β, °	c, Å/ γ, °	Syn. *	Structural Complexity Parameters, Bits per Atom/Bits per Unit Cell		Ref.
Edge-sharing interpolyhedral linkage									
Layers with clusters of uranyl polyhedra									
	Iriginite topology								
42	$[Ca(UO_2)(Mo_2O_7)_2]$	*P*-1	13.239(5)/90.00(4)	6.651(2)/90.38(4)	8.236(3)/120.16(3)	SQT[600]	4.392/184.477	4.459/196.215	[75]
43	$[(UO_2)(Mo_2O_7)(H_2O)_2]$	*C*2/*c*	35.071(6)/90	6.717(1)/90.069(6)	11.513(2)/90	HT[230]	4.301/326.842	4.684/468.386	[76]
	Layers of miscellaneous topologies								
44	$Ag_6[(UO_2)_3O(MoO_4)_5]$	*C*2/*c*	16.4508(14)/90	11.3236(14)/100.014(8)	12.7418(13)/90	SS[650]	4.215/295.05	4.431/363.319	[77]
45	$K_2[UO_2(Mo_2O_7)_2]$	*P*2$_1$/*c*	9.0775(5)/90	4.9444(2)/106.912(6)	15.2017(10)/-	SS[900]/HP	3.440/144.477	3.567/164.084	[5]
46	$(NH_4)_4((UO_2)_2(H_2O)_3UMo_{12}O_{42})(H_2O)_{18}$	*P*-1	11.429(2)/84.58(2)	14.359(3)/87.96(2)	16.491(3)/87.38(2)	Aq	6.016/770.000	6.625/1298.483	[78]
	Phosphuranylite topology, $6^15^24^23^2$								
47	$C(NH_2)_3(UO_2)(OH)(MoO_4)$	*P*2$_1$/*c*	15.411(1)/90	7.086(1)/113.125(2)	18.108(1)/90	HT[180]	4.322/345.754	5.248/797.685	[72]
Layers with chains of uranyl polyhedra									
48	$Cs_4[(UO_2)_3O(MoO_4)_2(MoO_5)]$	*P*1	7.510(2)/79.279(5)	7.897(2)/81.269(5)	9.774(2)/87.251(5)	SS[850]	4.700/122.211	4.907/147.207	[58]
	$5^34^33^2$-I								
49	$CsNa_3[(UO_2)_4O_4(Mo_2O_8)]$	*P*-1	6.4655(13)/84.325(10)	6.9057(10)/77.906(9)	11.381(2)/80.230(9)	SS[950]	3.700/96.211	3.974/119.207	[79]
	$5^24^33^2$								
50	$Ag_{10}[(UO_2)_8O_8(Mo_5O_{20})]$	*C*2/*c*	24.672(2)/90	23.401(2)/94.985(2)	6.7932(4)/90	SS[650]	4.850/552.949	5.176/703.895	[80]
51	$K_2Na_8(UO_2)_8(Mo_4O_{24})[(S,Mo)O_4]$	*C*2/*c*	24.282(4)/90	12.1170(18)/106.33(1)	13.6174(17)/90	SS[700]	4.892/567.526	5.117/695.895	[81]
52	$Cs_2Na_8[(UO_2)_8O_8(Mo_5O_{20})]$	*Ibam*	6.8460(2)/90	23.3855(7)/90	12.3373(3)/-	SS[950]	3.479/201.763	3.793/257.947	[79]
	$5^34^33^2$-II								
53	$Rb_2[(UO_2)_2(MoO_4)O_2]$	*P*2$_1$/*c*	8.542(1)/90	15.360(2)/104.279(3)	8.436(1)/90	SS[1000]	3.700/192.423	3.907/234.413	[82]
54	$K_2(UO_2)_2(MoO_4)O_2$	*P*2$_1$/*c*	8.2498(9)/90	15.337(2)/104.748(5)	8.3514(9)/90	Flx[950]	3.700/192.423	3.907/234.413	[83]
Layers with 2D linkage of uranyl polyhedra									
	$5^84^53^6$								
55	$K_8[(UO_2)_8(MoO_5)_3O_6]$	*P*4/*n*	23.488(3)/90	23.488(3)/90	6.7857(11)/90	Flx[950]	4.682/908.383	4.891/1105.360	[83]

Table 2. *Cont.*

No.	Chemical Formula	Sp. Gr.	a, Å/ α, °	b, Å/ β, °	c, Å/ γ, °	Syn. *	Structural Complexity Parameters, Bits per Atom/Bits per Unit Cell		Ref.
	$5^84^33^5$								
56	$Tl_2[(UO_2)_2O(MoO_5)]$	$P2_1/n$	8.2527(3)/90	28.5081(12)/104.122(1)	9.1555(4)/90	SS[650]	4.700/488.846	4.907/588.827	[84]
				FRAMEWORKS					
				Vertex-sharing interpolyhedral linkage					
57	$Ca[(UO_2)_6(MoO_4)_7(H_2O)_2](H_2O)_{7.6}$	$C222_1$	11.3691(9)/90	20.0311(5)/90	23.8333(18)/90	HT[230]	4.800/527.95	5.800/1275.899	[85]
57a	$Ca((UO_2)_6(MoO_4)_7(H_2O)_2)(H_2O)_{15}$ **	$C222_1$	11.3691(9)/90	20.0311(15)/90	23.8333(18)/90	HT[230]	4.800/527.95	6.016/1540	[85]
58	α-$Cs_2[(UO_2)_2(MoO_4)_3]$	$Pna2_1$	20.4302(15)/90	8.5552(7)/90	9.8549(7)/90	HT[180]	4.492/368.955	4.524/416.168	[73]
59	$Rb_2[(UO_2)_2(MoO_4)_3]$	$Pna2_1$	20.214(1)/90	8.3744(4)/90	9.7464(5)/90	SS[700]	4.492/368.955	4.524/416.168	[59]
60	$Tl_2[(UO_2)_2(MoO_4)_3]$	$Pna2_1$	20.1296(9)/90	8.2811(4)/90	9.7045(4)/90	SS[600]	4.492/368.955	4.524/416.168	[86]
61	α-$[(UO_2)(MoO_4)(H_2O)_2]$	$P2_1/c$	13.612(5)/90	11.005(4)/113.05(3)	10.854(3)/90	HT[190]	4.170/300.235	4.755/513.528	[87]
62	$Sr[(UO_2)_6(MoO_4)_7(H_2O)_{15}]$	$C222_1$	11.166(5)/90	20.281(10)/90	24.061(12)/90	HT	4.800/527.95	5.311/828.523	[88]
63	$Mg[(UO_2)_6(MoO_4)_7](H_2O)_{18}$	$C222_1$	11.313(5)/90	20.163(10)/90	23.877(11)/90	HT	4.800/527.95	5.416/909.909	[88]
64	$(NH_4)_2[(UO_2)_6(MoO_4)_7(H_2O)_2]$	$Pbcm$	13.970(1)/90	10.747(1)/90	25.607(2)/90	HT[180]	4.945/1087.899	5.196/1371.720	[89]
65	$Rb_2[(UO_2)_6(MoO_4)_7(H_2O)_2]$	$Pbcm$	13.961(2)/90	10.752(2)/90	25.579(4)/90	HT[230]	4.945/1087.899	5.192/1349.816	[59]
66	$Cs_2[(UO_2)_6(MoO_4)_7(H_2O)_2]$	$Pbcm$	13.990(2)/90	10.808(1)/90	25.671(3)/90	HT[230]	4.945/1087.899	5.192/1349.816	[89]
67	$Ag_2[(UO_2)_6(MoO_4)_7(H_2O)_2](H_2O)_2$	$Pbcm$	14.1309(9)/90	10.6595(7)/90	25.8281(16)/90	HT[220]	4.945/1087.899	5.264/1431.790	[90]
68	$K_{2.98}[(UO_2)_6(OH)_2(MoO_4)_6(MoO_3OH)]$	$Pbcm$	13.9807(12)/90	10.7427(9)/90	25.517(2)/90	SS[900]/HP	4.945/1087.899	5.152/1298.275	[5]
69	$Na_2UO_2(MoO_4)_2(H_2O)$	$P2_12_12_1$	8.6005(16)/90	10.749(2)/90	11.086(2)/90	HT[200]	3.700/192.423	4.170/200.235	[91]
70	$Ba[(UO_2)_3(MoO_4)_4(H_2O)_4]$	$Pbca$	17.797(8)/90	11.975(6)/90	23.33(1)/90	HT	4.907/1177.654	5.285/1649.045	[92]
71	$Mg[(UO_2)_3(MoO_4)_4(H_2O)_8]$	$Cmc2_1$	17.105(8)/90	13.786(6)/90	10.908(5)/90	HT[240]	4.115/255.160	4.996/579.526	[93]
72	$Zn[(UO_2)_3(MoO_4)_4(H_2O)_8]$	$Cmc2_1$	17.056(8)/90	13.786(6)/90	10.919(5)/90	HT[240]	4.115/255.160	4.752/456.156	[93]
73	$(NH_4)_4[(UO_2)_5(MoO_4)_7](H_2O)_5$	$P6_1$	11.4067(5)/90	11.4067(5)/90	70.659(5)/120	HT[180]	5.644/1693.157	6.066/2438.568	[94]
74	$[(C_2H_5)_2NH_2]_2[(UO_2)_4(MoO_4)_5(H_2O)](H_2O)$	$P6_522$	11.3612(13)/90	11.3612(13)/90	52.698(8)/120	HT[220]	4.524/1248.503	4.807/1615.271	[95]
75	$[(UO_2)(MoO_4)]$	$P2_1/c$	7.202(3)/90	5.484(2)/104.54(2)	13.599(2)/90		3.000/96.000	3.000/96.000	[96]

Table 2. *Cont.*

No.	Chemical Formula	Sp. Gr.	*a*, Å/ α, °	*b*, Å/ β, °	c, Å/ γ, °	Syn. *	Structural Complexity Parameters, Bits per Atom/Bits per Unit Cell		Ref.
				Edge-sharing interpolyhedral linkage					
76	$K_2[(UO_2)_2(Mo^{(VI)}{}_4Mo^{(IV)}(OH)_2)O_{16}]$	*P*-1	5.0468(9)/88.456(10)	6.8982(7)/69.815(15)	7.2414(12)/69.493(12)	SS[900]/HP	3.125/50.000	2.974/44.603	[5]
77	$Li_4[(UO_2)_{10}O_{10}(Mo_2O_8)]$	*P*2$_1$/*c*	7.9426(4)/90	19.9895(9)/90.575(2)	10.0796(5)/90	SS[870]	4.684/468.386	4.792/517.528	[97]
78	$K_5[(UO_2)_{10}MoO_5O_{11}OH]H_2O$	*P*1	8.0728(5)/111.118(6)	11.0224(7)/102.845(5)	11.4744(6)/104.506(6)	SS[900]/HP	5.585/268.078	5.728/303.580	[5]

* Synthesis data. SS[T] corresponds to solid state synthesis at maximum reported temperature T (°C). SS[T]/HP corresponds to high temperature/high pressure solid state synthesis. HT[T] corresponds to hydrothermal synthesis at maximum reported temperature T (°C) (HTwA[T] is deciphered as hydrothermal synthesis with acidified mother solution). Flx means usage of molten flux in a synthesis. Aq is deciphered as synthesis based on evaporation at room temperature. SQT is the Sealed Quartz Tube method. ** **57** and **57a** are supposed to be the same compound, but **57a** has a mistake in the deposited crystallographic information file (CSD 250347).

3. Results and Discussion

3.1. Uranyl Molybdate Minerals

Uranyl molybdate minerals (Table 1) are common in roll-front deposits (uranium deposit in Tengchong County, Yunnan, China) and other deposits where uraninite and the weathering of Mo-bearing minerals occurs [6]. They can form on granites [45], albitites [41], and on quartz veins [47], sometimes as pseudomorphs after brannerite and uraninite [41,51]. These minerals are commonly found in association with other uranyl molybdates, uranyl silicates, uranyl hydrates, molybdenite, quartz, baryte, uraninite, brannerite, pirite, gypsum, and others.

The geography of discoveries of minerals that contain U and Mo is wide; there is no locality that would be characterized by numerous findings in comparison with others. Their crystals are found in different types of uranium deposits, including intrusive (Radium Hill area, Olary Province, South Australia), vein (Kyzylsai Mo-U deposit, Chu-Ili Mountains, Moiynkum, Jambyl Region, Kazakhstan), volcanic (Oktyabr'skoe Mo-U Deposit, Strel'tsovskoe Mo-U ore field, Krasnokamensk, Krasnokamensky District, Zabaykalsky Krai, Russia), and sedimentary roll-front (Tengchong County, Baoshan, Yunnan, China) deposits.

Molybdenum in these minerals is present in the form of hexavalent ion (Mo^{6+}), while uranium may be in a mixed oxidation state (U^{4+} and U^{6+}). Uranyl molybdates coexist as fine-grained aggregates [98,99] and colloform growths [41].

Nine minerals of U and Mo are known, but crystal structures have only been reported for five of them: umohoite [37], deloryite [33], baumoite [45], tengchongite [47], and iriginite [43]. The lack of structural information is likely due to the peculiarities of the crystals' morphology and their quality for structure analysis.

The first uranyl molybdate minerals were discovered in the middle of 20th century. The first mention of these minerals occurs in 1951 in the manuscript of Epshtein [42]. The minerals described were iriginite and moluranite, found as thin crusts and sometimes pseudomorphs after brannerite in crushed albitites [41]. The locality of the discovery was Aleksandrovskii Golets Mo-U occurrence, Aldan Shield, U.S.S.R.

The second finding was mineral umohoite, $[(UO_2)(MoO_4)(H_2O)](H_2O)$ [34], reported in 1953 in USA, and named as a reflection of its elemental composition (uranium, molybdenum, hydrogen, and oxygen). It forms rosettes of black or dark green tabular plates.

In 1958, magnesium uranyl molybdate cousinite was discovered, and its structure remains unknown [55]. It was found in Shinkolobwe mine in Congo as black blade-like crystals.

The minerals calcurmolite and mourite were described in 1959 and 1962, respectively. They were named on the same principle as umohoite. Calcurmolite occured as prismatic crystals in radial bright yellow aggregates, sometimes as pseudomorphs after uraninite [51]. They were found in the Sokh-Karasu area, Armenia. Mourite was found in the hypergenesis zone of the Kyzylsai Mo-U deposit, Kazakhstan, as fine-grained violet aggregates and in thin crusts [49].

The next finding was the uranium molybdate mineral sedovite, named after Georgii Sedov, a Russian polar explorer [57]. It forms in alkaline conditions and is much less common than uranyl molybdates, the formation of which occured later. It was found in the hypergene zone of the Kyzylsai Mo-U deposit in Kazakhstan, together with other uranium minerals and uranyl molybdates.

Tengchongite was found in 1986 at a uranium occurrence in Tengchong County, Yunnan, China. It is the second calcium uranyl molybdate after calcurmolite. The mineral was named after the locality where it was found as mica-schistose crystals within the contact of migmatite and migmatic gneiss [46].

Deloryite, the first copper uranyl molybdate, was discovered in 1992. It was found in Cap Garonne mine near Le Pradet, Var, France, and named after mineral collector Jean Claude Delory [31]. It occurred as rosettes of green crystals.

The most recent mineral discovered was baumoite (barium uranyl molybdate). It was found in 2019 near Radium Hill, South Australia [45]. The mineral was named for its composition, which includes barium, uranium, and molybdenum. Baumoite occurred as yellow to orange thin crusts of prismatic crystals on weathered granite as the result of barite alteration.

3.2. Synthetic Uranyl Molybdates

It should be noted that most of the known uranyl molybdates were synthesized in laboratories. The amount of synthetic phases is nearly one order larger than the number of mineral phases, with the ratio of 69:9. The first uranyl molybdate compound synthesized and structurally characterized was $[(UO_2)(MoO_4)]$ [96]. The great contribution to the understanding to the structural diversity of uranyl molybdates was offered by S.V. Krivovichev and P. Burns [7, 58, 59, 60, 65, 69]. More than 30 compounds were synthesized and structurally characterized by their scientific groups.

Synthetic uranyl molybdates can be divided into two groups: pure inorganic and mixed organic-inorganic compounds. The group of organic-inorganic compounds is much smaller; it includes only eight compounds. The latter group, inorganic compounds, consists of 61 uranyl molybdates.

Nearly half of known inorganic uranyl molybdates were synthesized using hydrothermal techniques (35 compounds), and only four of them were synthesized in slightly specific conditions: the mother liquid solution for the compounds **14**, **23**, **27**, and **28** was previously acidified with HNO_3. The temperature for the experiments ranges from 120 to 280 °C and the duration of experiments was from 1 h to 80 days. Uranyl nitrate hexahydrate, $(UO_2)(NO_3)_2\cdot6H_2O$, and uranyl acetate hexahydrate, $UO_2(CH_3COO)_2\cdot6H_2O$, were used as the U-bearing component in most of the experiments. In some syntheses, uranium oxide UO_3 (**16**, **24**, **67**), uranyl hydroxide $UO_2(OH)_2$ (**61**), and uranyl molybdate dihydrate $UO_2MoO_4\cdot2H_2O$ (**62**, **63**, **70**, **71**, **71**, **72**) were used as the source of uranium. The source of Mo in these experiments was usually MoO_3, which was substituted in some cases by $Na_2MoO_4\cdot4H_2O$ (**14**, **22**, **23**, **26**, **35**), $(NH_4)_6Mo_7O_{24}$ (**64**, **73**), Na_2MoO_4 (**27**, **69**), $SrMoO_4$ (**62**), $BaMoO_4$ (**70**), $MgMoO_4$ (**63**, **71**), or $ZnMoO_4$ (**72**).

Twenty-nine compounds among the synthetic uranyl molybdates were synthesized by solid state reactions in a temperature range of 600–1000 °C and duration ranges from 24 to 185 h. Uranyl oxide, UO_3, was used as the U-bearing reagent in a large number of these experiments, but in some of them $UO_2(CH_3COO)_2\cdot2H_2O$ (**11**, **15**, **48**, **49**, **51**, **52**), $(UO_2)(NO_3)_2\cdot6H_2O$ (**45**, **68**, **76**, **78**), and U_3O_8 (**22**) were used. Molybdenum oxide was used as the source of Mo^{6+} ion for all compounds, synthesized by this method.

Two uranyl molybdates (**54**, **55**) were synthesized by the flux method. U_3O_8 and MoO_3 were used as initial reagents and potassium carbonate was used as a flux compound.

Compounds **32** and **46** were obtained via evaporation at room temperature technique. In both experiments uranyl nitrate was used, while $Na_2MoO_4\cdot4H_2O$ was added to the experimental solution of **32** and $UO_2MoO_4\cdot2H_2O$ for **46**.

Only one uranyl molybdate was synthesized via sealed quartz tube method (**40**) using uranyl and molybdenum oxides.

All mixed organic-inorganic uranyl molybdate compounds were obtained via the hydrothermal method at a temperature range of 180–220 °C and a duration rang from 24 to 65 h. Uranyl acetate dihydrate was used as the U reagent in seven experiments; in the case of **38**, $(UO_2)(NO_3)_2\cdot6H_2O$ was used. Molybdenum oxide was used as the source of Mo for preparation of **31**, **41**, **39**, and **74**, while **34**, **36**, **40**, and **47** were synthesized using $(NH_4)_2Mo_2O_7$.

The dominant methods of obtaining synthetic inorganic uranyl molybdates are the hydrothermal and solid-state techniques. The temperature chosen for hydrothermal syntheses is not higher than 280 °C, but, on the other hand, is much higher for solid-state reactions: about 600–1000 °C. For mixed organic-inorganic uranyl molybdates, only the hydrothermal method is applicable. The temperature of obtaining compounds is not higher than 220 °C. Only a few compounds were synthesized via different techniques, including aqueous, flux, or sealed quartz tube methods.

The reagents used for the experiments are quite different. The only appropriate way is to consider those predominantly used. Uranyl nitrate and uranyl acetate are the dominant sources of uranium in hydrothermal experiments and uranyl oxide in solid-state reactions.

3.3. Topological Analysis

There are only four synthetic compounds, upon which crystals structures are based on the uranyl molybdate finite clusters (Figure 1a–d). Topologies of their U-bearing substructural units are rather simple but are quite rare. The topologies of both the cc0–1:4–1 and cc0–1:4–2 types have been observed in the crystal structures of uranyl sulfate minerals belakovskiite and bluelizardite, respectively [26].

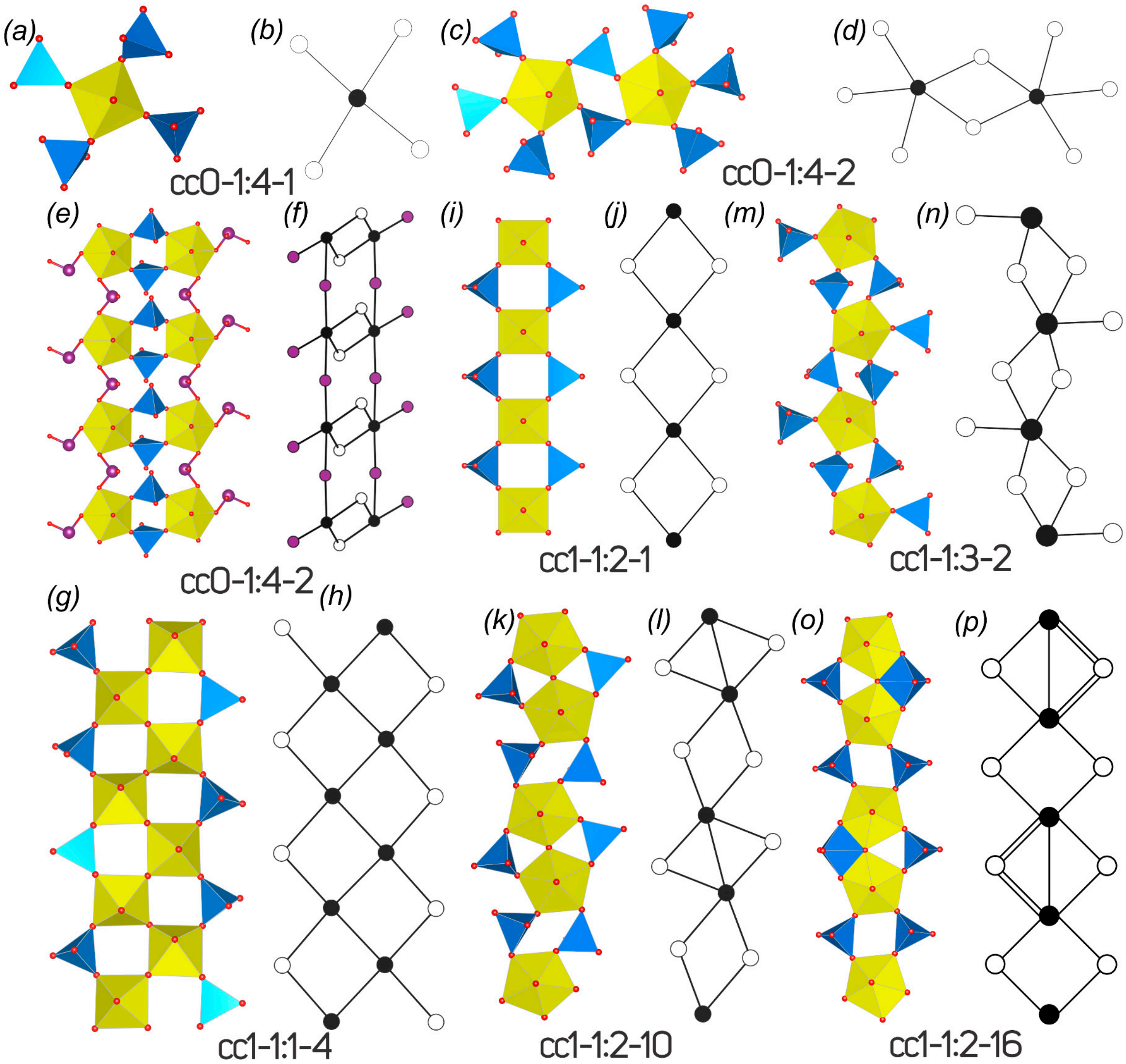

Figure 1. 0D (**a**–**f**) and 1D (**g**–**p**) complexes in the crystal structures of uranyl molybdates. See text for details). Legend: U-bearing coordination polyhedra = yellow, Mo-bearing coordination polyhedra = blue, O atoms = red; black nodes = U atoms, white nodes = Mo atoms.

The structural complex of the only mineral, which is based on infinite uranyl molybdate chains, has the very common topology of the cc1–1:1–4 type (Figure 1g,h). It has been observed among both uranyl selenite and uranyl sulfate minerals [26,27]. In terms of its structural architecture, deloryite can be considered as an analogue of the uranyl selenite mineral derriksite [27]. Uranyl molybdate chains are located along the (010) vector and are separated by Cu-centered tri-octahedral layers parallel to (100).

Uranyl molybdate chains of the cc1–1:3–2 topology were found in the structure of only two synthetic compounds, **22** and **23**; however, the structure of another uranyl selenite mineral, demesmaekerite, is also based on this type of 1D complexes [27]. Topologies of the cc1–1:1–4, cc1–1:2–10, and cc1–1:2–16 types are even rarer. In particular, the last two have been found only among uranyl molybdates.

Almost half of the currently known uranyl molybdates are based on layered complexes (Tables 1 and 2; Figures 2–7). Moreover, the crystal structures of four out of five known natural compounds are also attributed to layered ones.

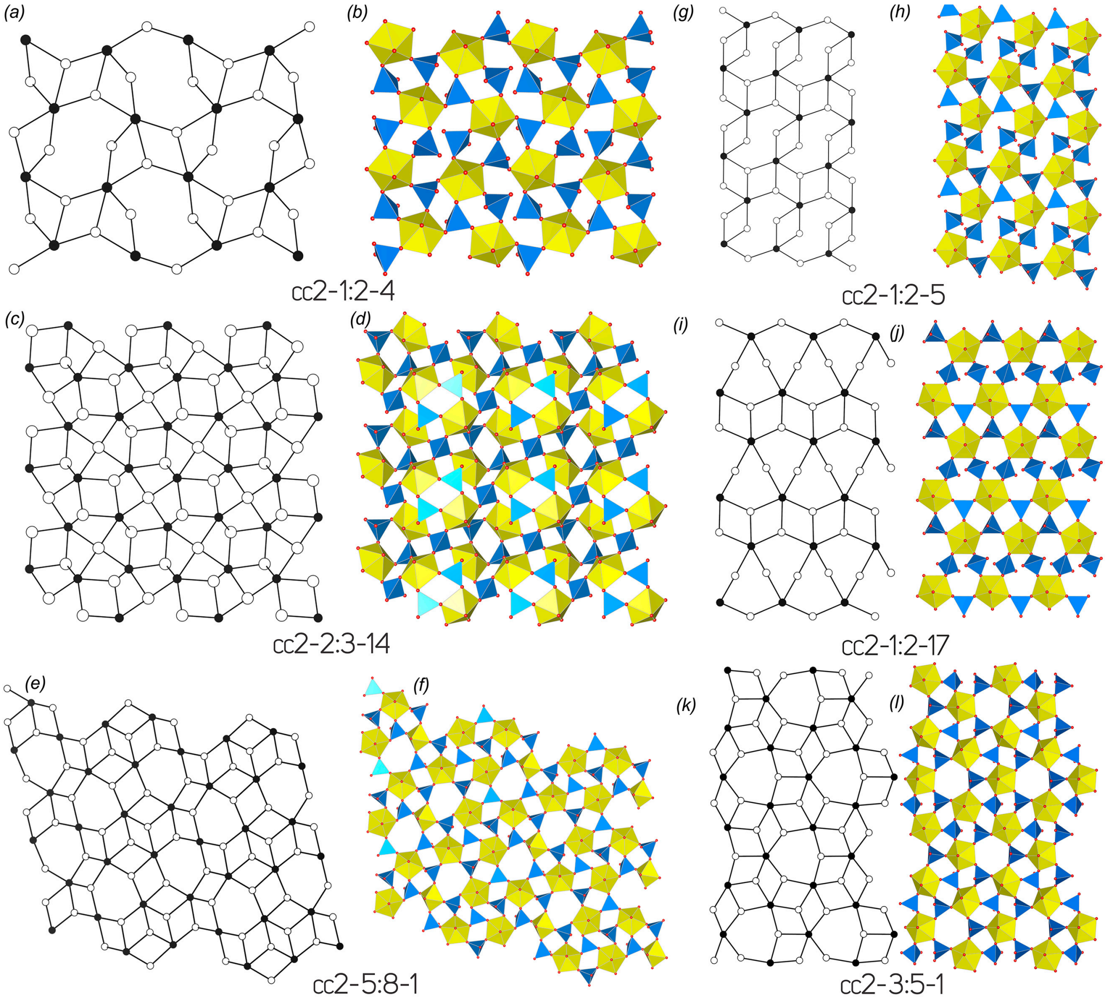

Figure 2. 2D complexes based on corner-sharing linkage and their respective graphs in the crystal structures of uranyl molybdates; see text and Tables 1 and 2 for details. Legend: see Figure 1.

The crystal structures of 10 compounds (**25**–**35**) are based on the cc2–1:2–4 topology (Figure 2a,b), which is highly common among uranyl oxysalt compounds. It is the most common topology among uranyl selenates and selenites [27]; nine known synthetic compounds belong to it. It is of interest that the cc2–1:2–5 topology (Figure 2g,h), is also formed by eight- and four-membered cycles, as in the previous type, but differs in their relative arrangement within the layer. Despite the relatively small topological difference, such layers were described in the structure of uranyl molybdate **36**.

One of the most common topologies among the U-bearing compounds, the edge-sharing interpolyhedral linkage (phosphuranylite type; Figure 3a,b) [12], have only been observed in compound **47**.

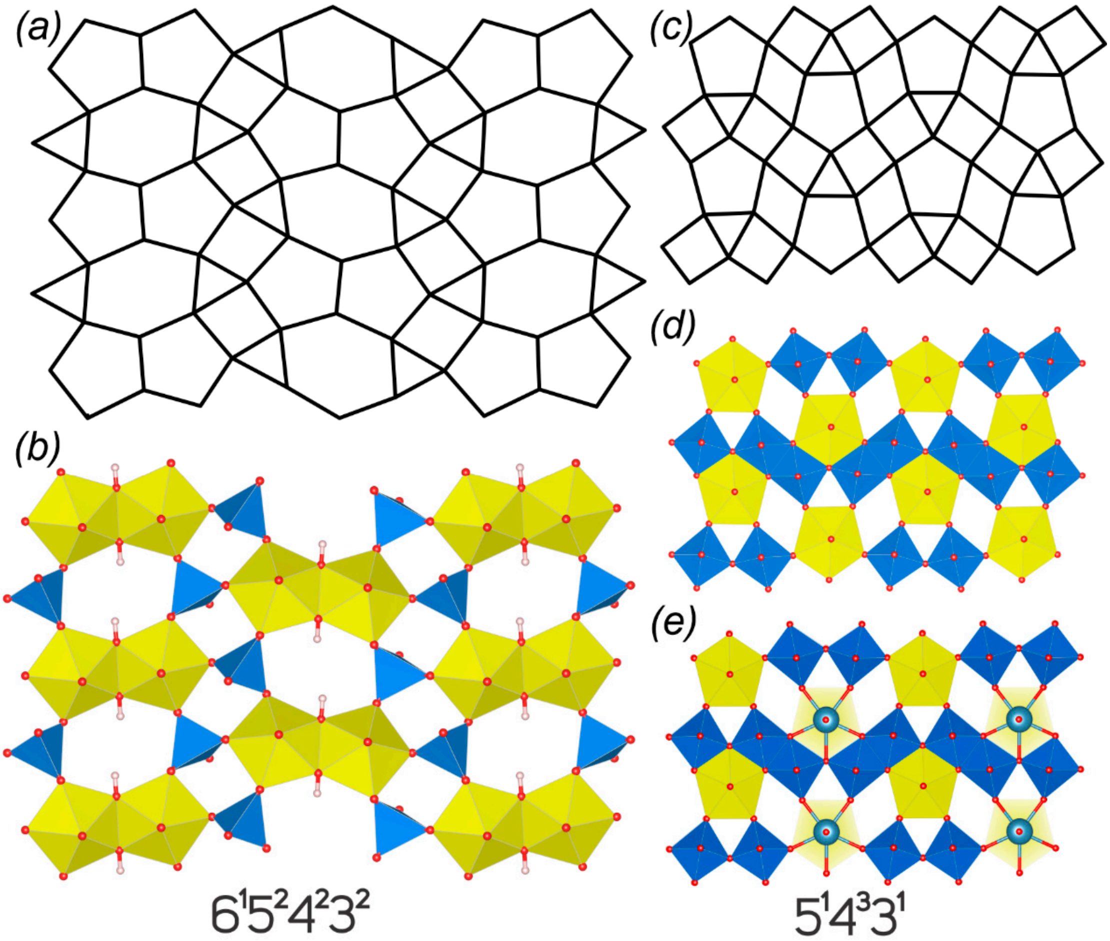

Figure 3. 2D complexes with edge-sharing interpolyhedral linkage of U and Mo coordination polyhedra based on clusters of uranyl polyhedra, and respective anion topologies; see text and Tables 1 and 2 for details. Legend: see Figure 1.

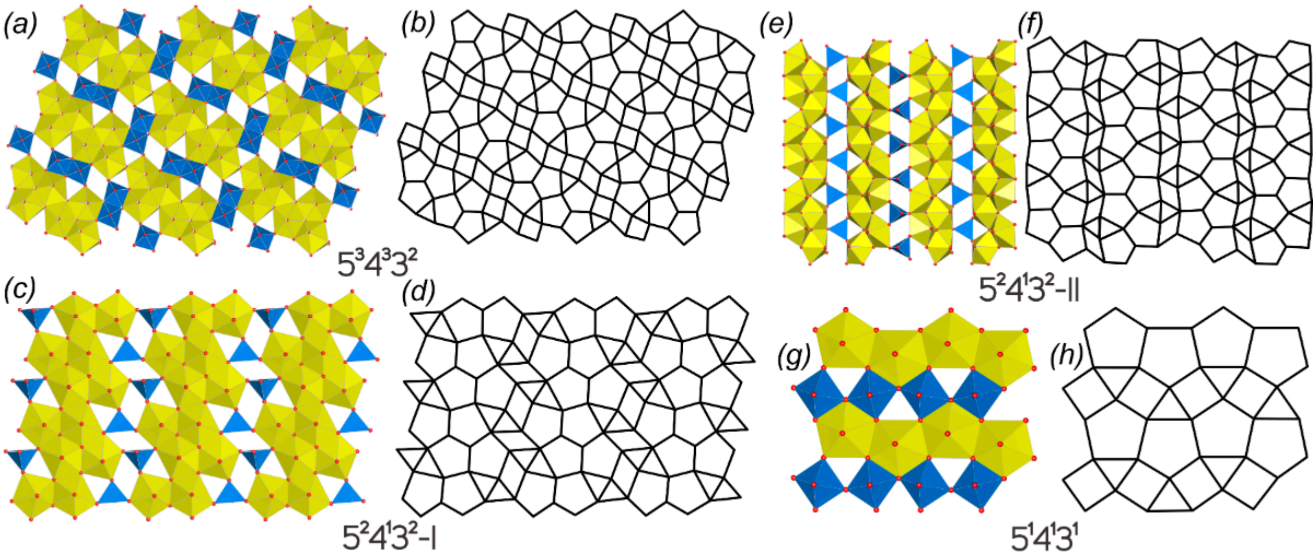

Figure 4. 2D complexes with edge-sharing interpolyhedral linkage of U and Mo coordination polyhedra based on chains of uranyl polyhedra, and respective anion topologies; see text and Tables 1 and 2 for details. Legend: see Figure 1.

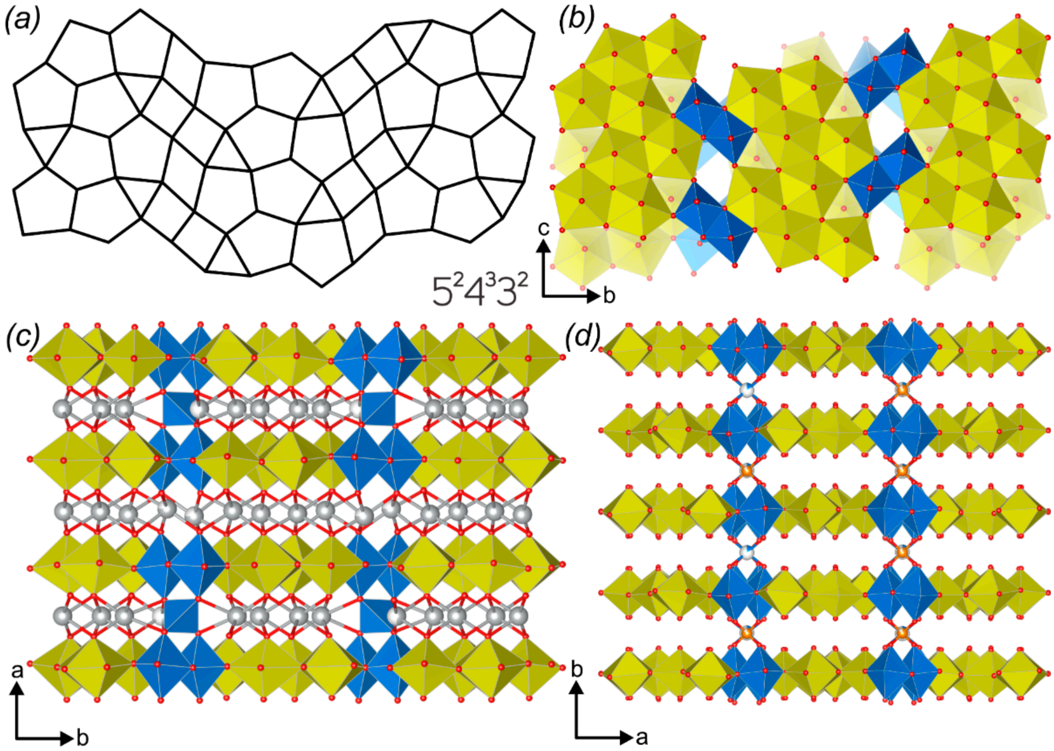

Figure 5. 2D complexes with edge-sharing interpolyhedral linkage of U and Mo coordination polyhedra based on chains of uranyl polyhedra of the $5^24^33^2$ type: anion topology (**a**), polyhedral representation of layers (**b**), and projection of **50** (**c**) and **51**–**52** (**d**) along the layers. Legend: see Figure 1.

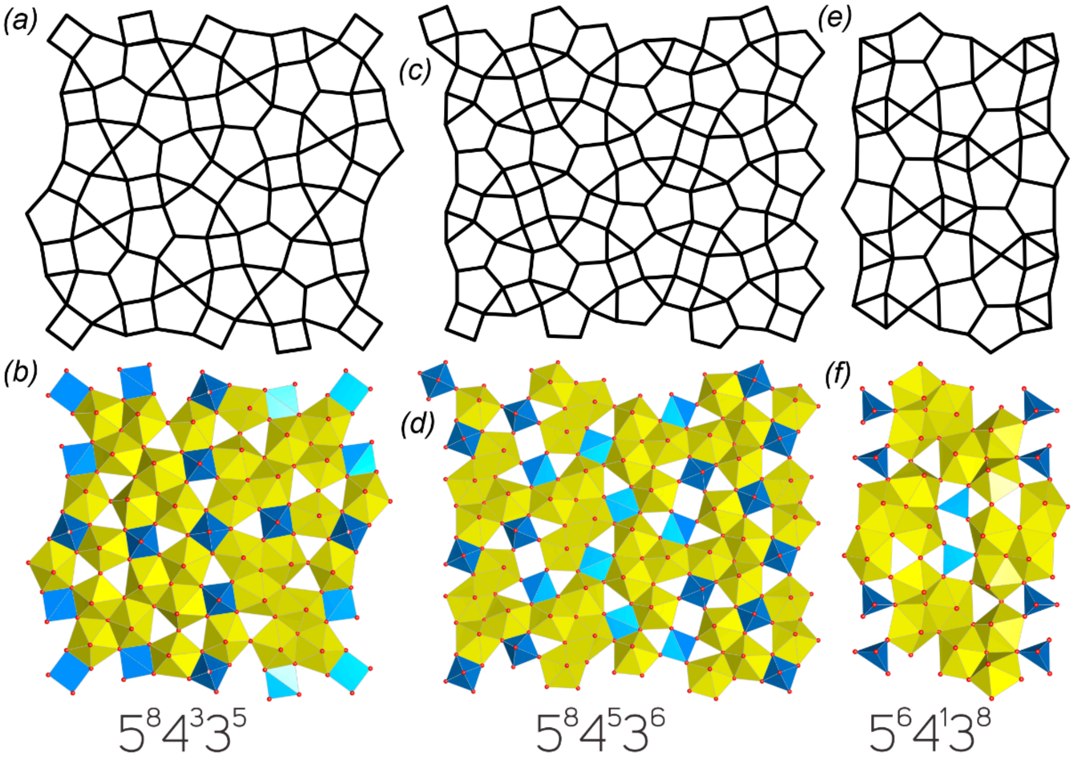

Figure 6. Layered complexes with edge-sharing interpolyhedral linkage of U and Mo coordination polyhedra based on 2D linkage of uranyl polyhedra, and respective anion topologies; see text and Tables 1 and 2 for details. Legend: see Figure 1.

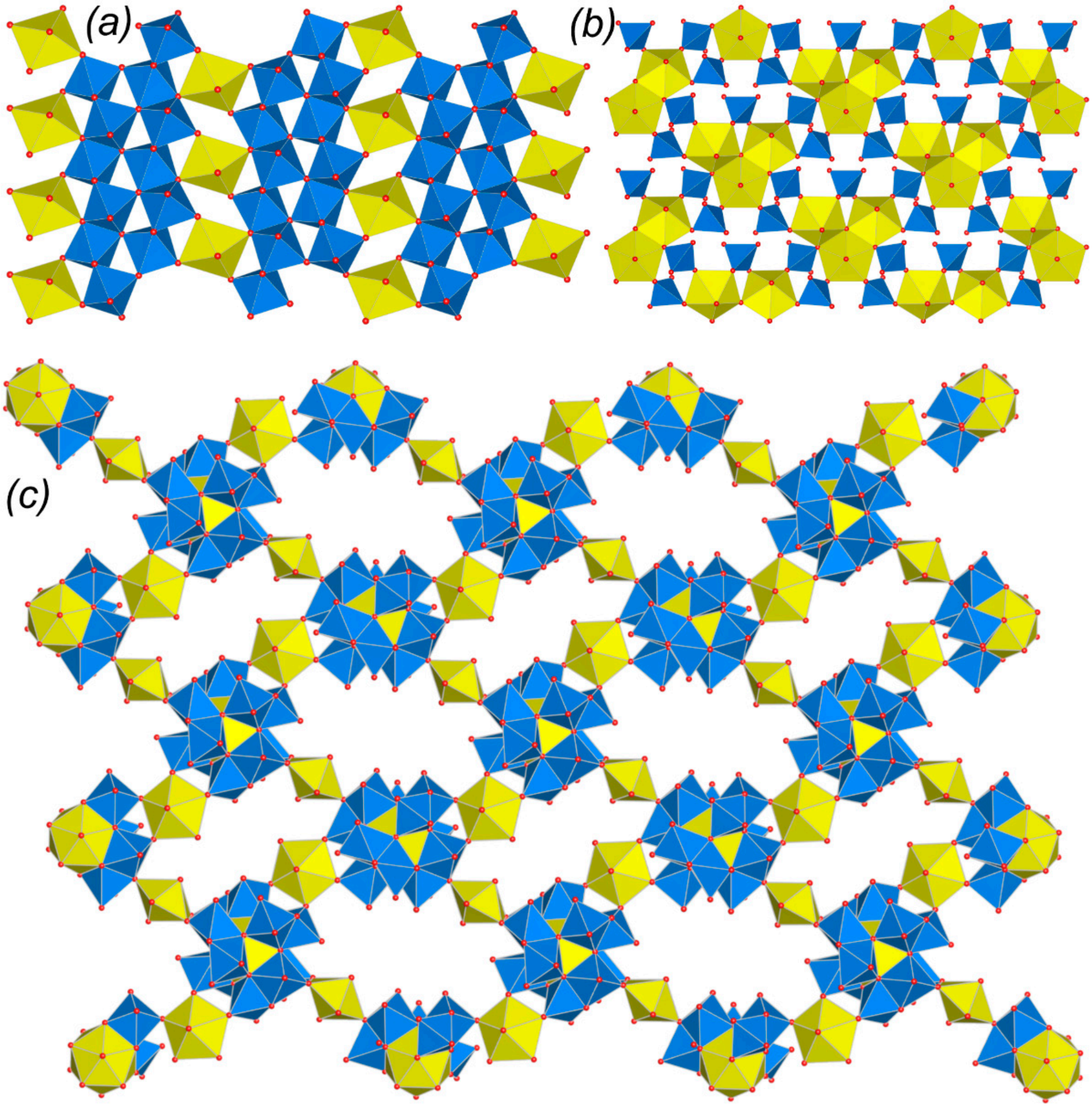

Figure 7. 2D complexes with vertex-sharing interpolyhedral linkage of U and Mo coordination polyhedra based on miscellaneous topologies in the structures of **45** (**a**), **44** (**b**) and **46** (**c**). Legend: see Figure 1.

The crystal structure of iriginite (**3**) is based on layers with the $5^1 4^3 3^1$ topology (Figure 3c). Moreover, in the case of this mineral and synthetic structure **43** all pentagons correspond to uranyl polyhedral (Figure 3d), then half of the pentagons are occupied by Ca^{2+} cations the structure of compound **42** (Figure 3e).

The crystal structures of **50**–**52** are based on the uranyl molybdate layers of the same topology (Figure 5), which was previously observed in uranyl tungstate [100]. It is of interest that despite topological similarity, all structures have distinctive features. Thus, the crystal structure of **50** (Figure 5c) has two alternating types of interlayer space. The first includes additional molybdate tetrahedra that link neighbor U-bearing layers. The second contains only Ag^+ ions. The crystal structures of **51** and **52** are more similar; their structures contain tetrahedral oxyanion links in each interlayer space (Figure 5d). Those links are sulfate-molybdate in **51** and pure molybdate in **52**.

It should be noted that there are few compounds in which structures have framework architecture; these are, in turn, based on layers of common topological types. For instance, the cc2–1:2–4 topology motif also appears in the projection of the U-Mo framework in crystal structure of **69** (Figure 8). In this case, the structural unit is formed by highly corrugated layers with a topology very close to the original. Moreover, at the junctions of the layers, a break in the layer topology with the transition to the next layer occurs. A similar arrangement can be found in the structures of **58–60** (Figure 9) and **75** (Figure 10).

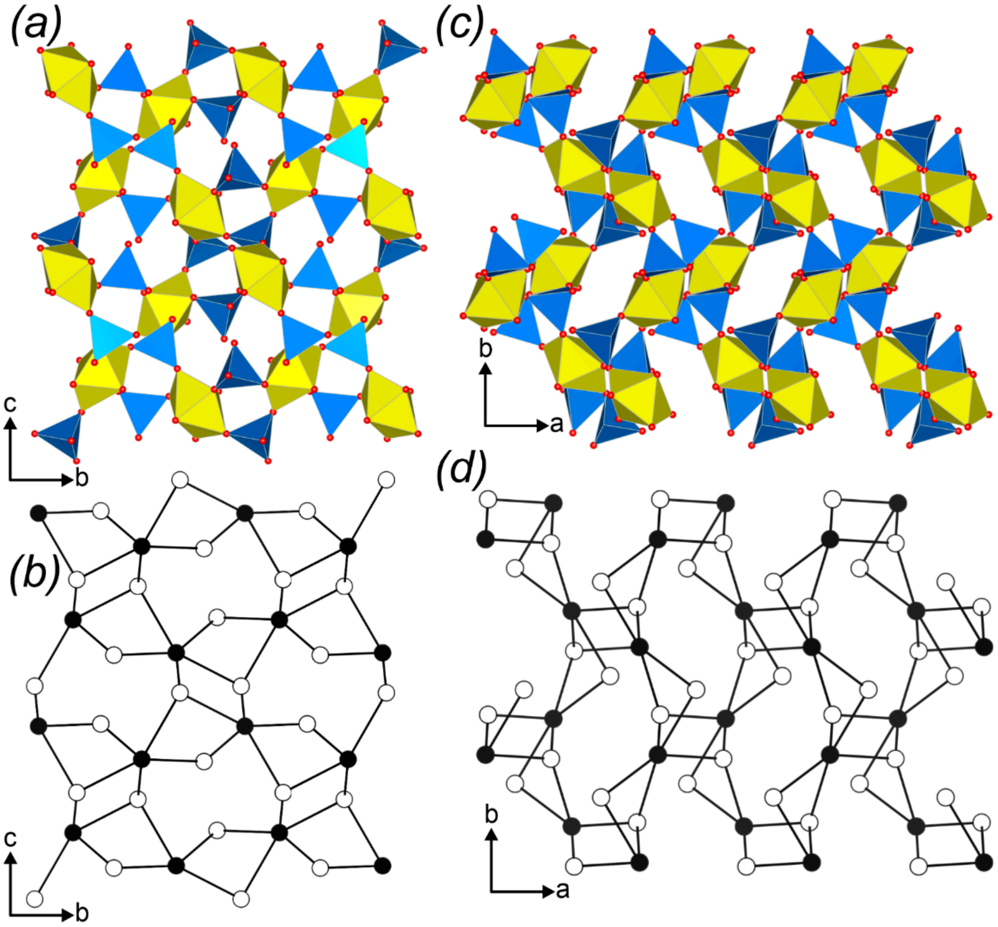

Figure 8. Framework architecture in the crystal structure of **69**, shown in two projections (**a**,**c**) with the corresponding graphs (**b**,**d**). Legend: see Figure 1.

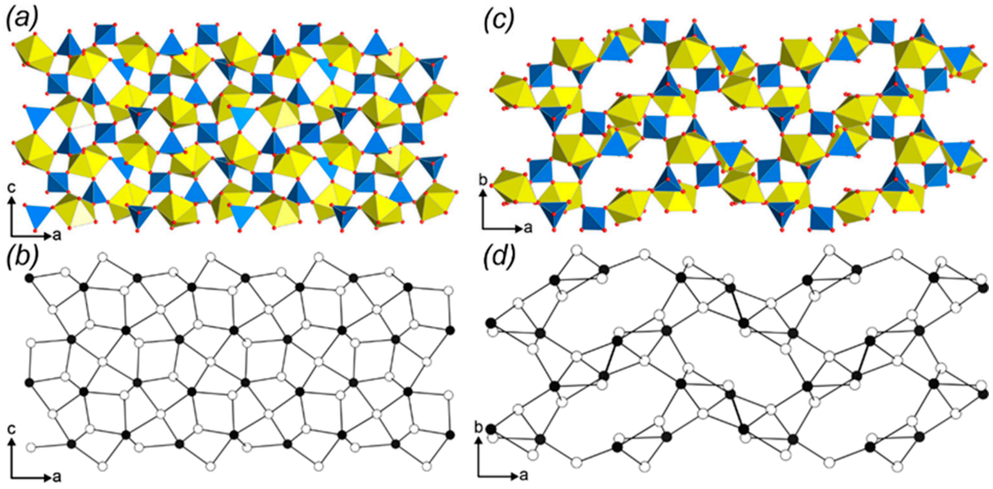

Figure 9. Framework architecture in the crystal structures of **58**–**60**, shown in two projections (**a**,**c**) with the corresponding graphs (**b**,**d**); the layered fragment (**a**,**b**) of this framework corresponds to the cc2–2:3–14 topological types. Legend: see Figure 1.

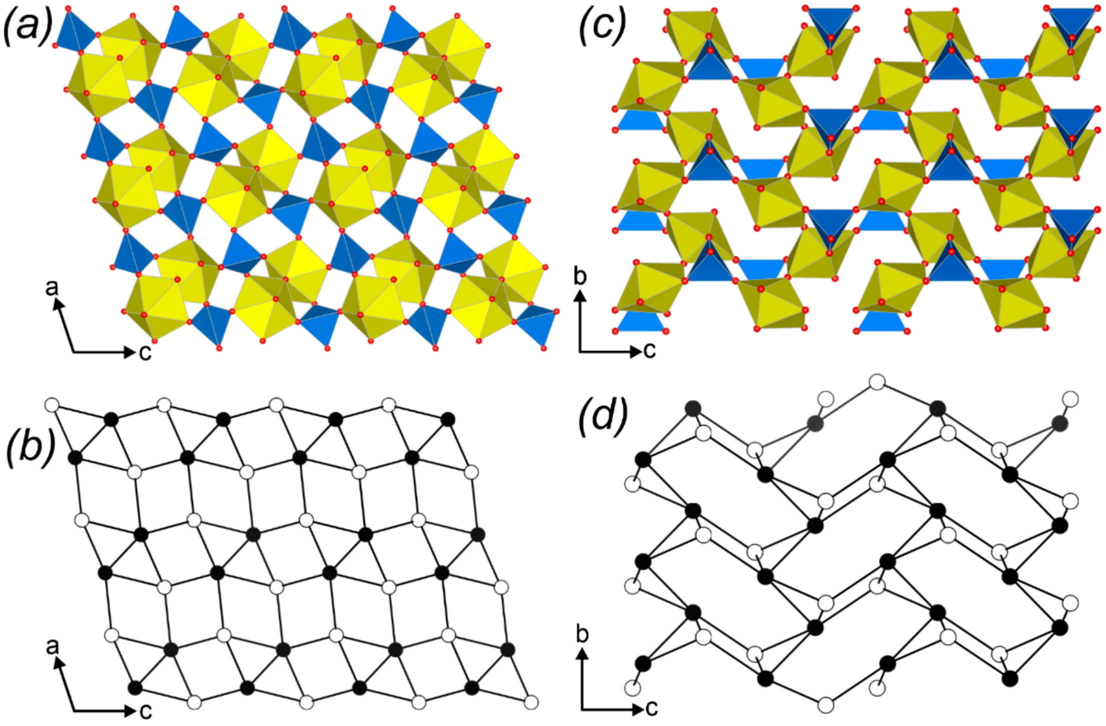

Figure 10. Framework architecture in the crystal structure of **75**, shown in two projections (**a**,**c**) with the corresponding graphs (**b**,**d**). Legend: see Figure 1.

The 2D uranyl molybdate complex of the cc2–2:3–14 topological type was described for compound **38** (Figure 2c,d). It can also be observed in the structures of **58**–**60**, where such layers are arranged in a highly undulated manner. The connection of layers into a framework construction occurs through uranyl molybdate linkers when layers approach each other at bends (Figure 9).

The crystal structure of **76** can also be described as a framework built by layers of unique topology (Figure 10). The structure of **78** is based on the edge-sharing layers linked together by additional U-centered polyhedra (Figure 11).

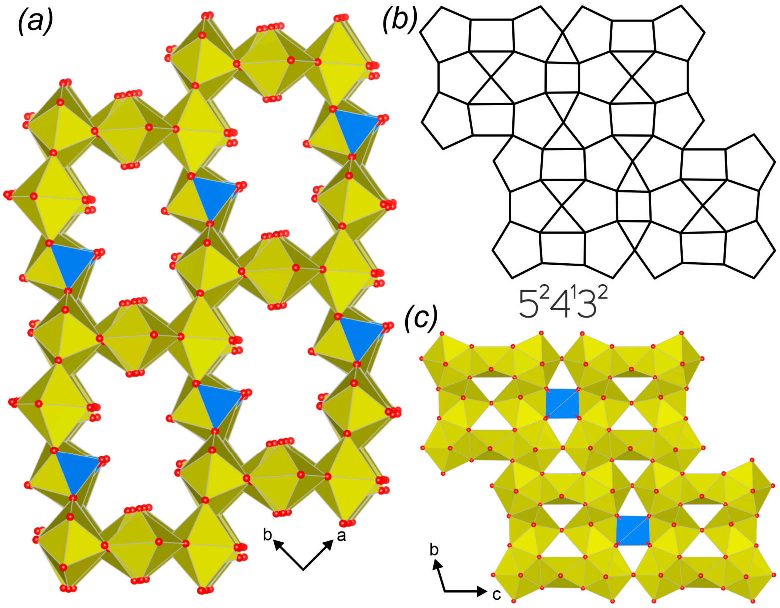

Figure 11. Framework architecture in the crystal structure of **78**, shown in two projections (**a**,**c**) with the corresponding anion topology (**b**). Legend: see Figure 1.

It should be noted that framework architecture appeared to be quite common within the uranyl molybdate crystal chemical diversity (Figures 11–14). Twenty-three uranyl molybdate compounds (one third of the total), of both natural and synthetic origin, have a framework structure, which is significantly more than for other groups of uranyl compounds. It may be the case that only uranyl silicates can compete for the palm. At the same time, this is not to say that topologies are very specific. On the contrary, some of them are known for other groups of uranyl compounds. For example, the microporous framework shown in Figure 11a was described in several uranyl sulfate crystal structures [101].

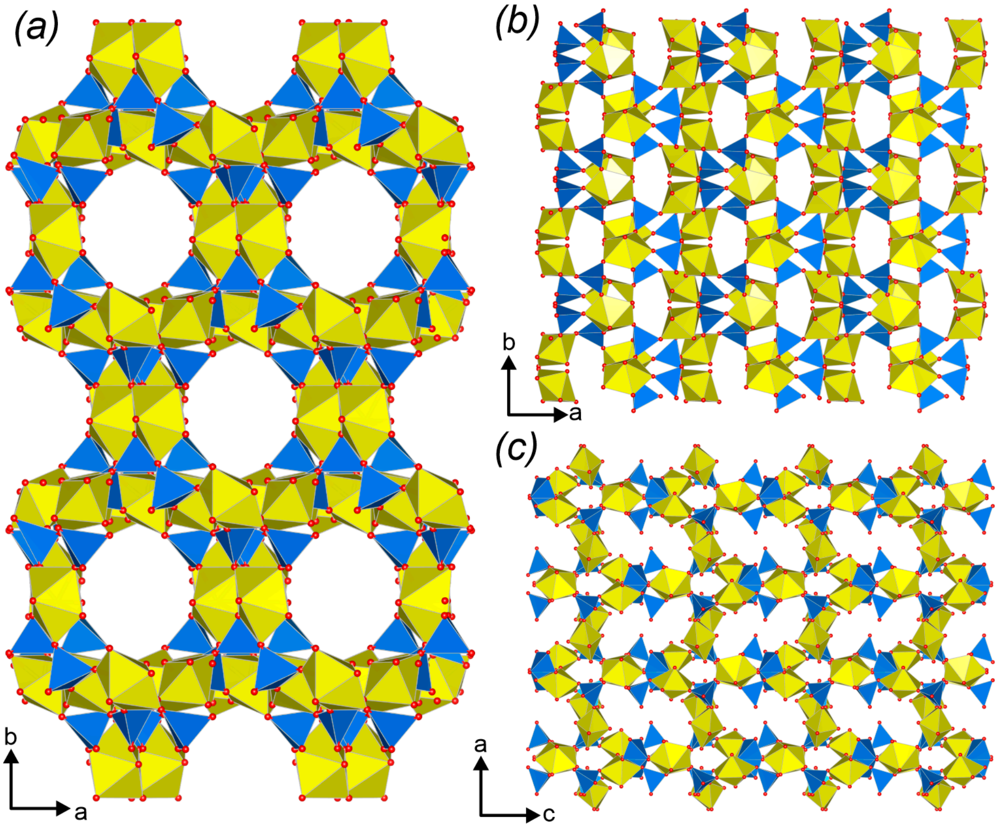

Figure 12. Framework architecture in the crystal structures of **57**, **62**–**63** (**a**), **61** (**b**), and **70** (**c**). Legend: see Figure 1.

3.4. Crystal Structures vs. Synthesis Conditions

Three out of four compounds with structures based on U-Mo finite clusters were obtained as a result of high-temperature solid-state syntheses. Compound **13**, obtained under high-temperature conditions, has a lower symmetry than another, compound **14**, based on the same cc0–1:4–2 cluster topology, but was obtained through medium-temperature hydrothermal synthesis. The symmetry of the cluster itself remains the same in both cases.

A similar tendency towards lower symmetry of compounds obtained by high-temperature solid state synthesis is observed for structures based on infinite chains. The crystal structure of **17** has a lower symmetry of the chain complex than that of **16**, obtained by the hydrothermal method. The structures of compounds **18**–**20**, based on the cc1–1:2–10 topological type of chains, crystallize in *P*-1 space group. At the same time, the chained complex in the structure of **20** has reduced symmetry relative to the other two compounds (Figure 15a,b). Different symmetries of chain complexes are also observed in the structures of compounds **22** and **23** (Figure 15c and Figure 15d, respectively). In the structure of **23**, the U-Mo chains are distorted relative to the almost planar configuration in structure of **22** and have a larger translation periodicity.

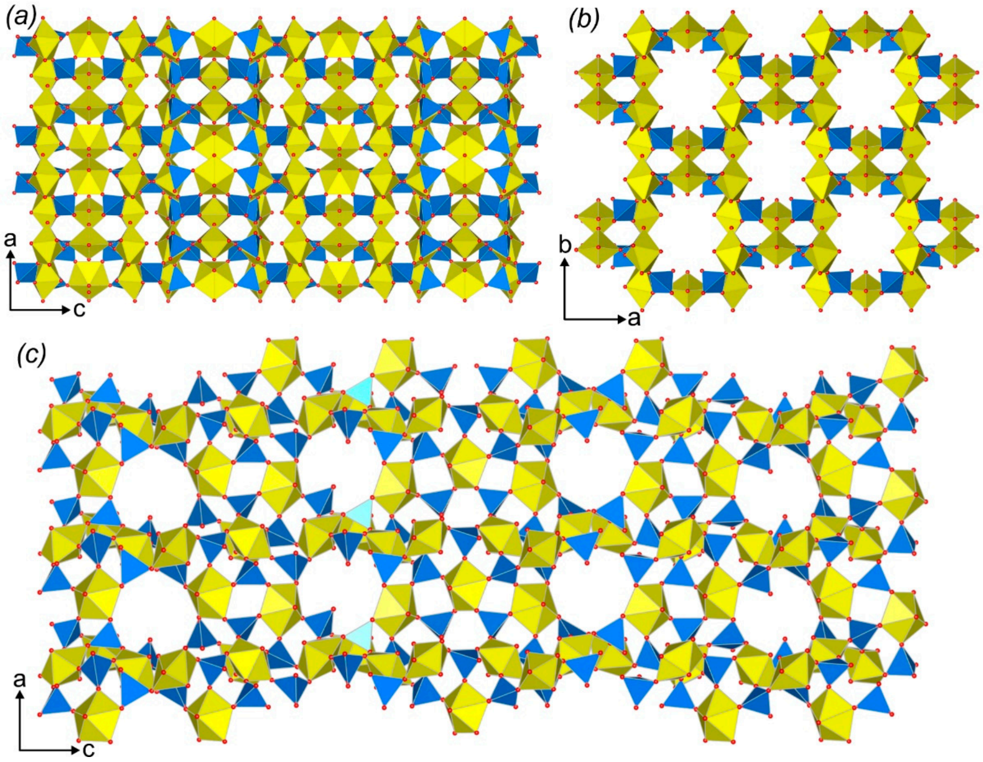

Figure 13. Framework architecture in the crystal structures of **64–68** (**a**), **71-72** (**b**), and **73** (**c**). Legend: see Figure 1.

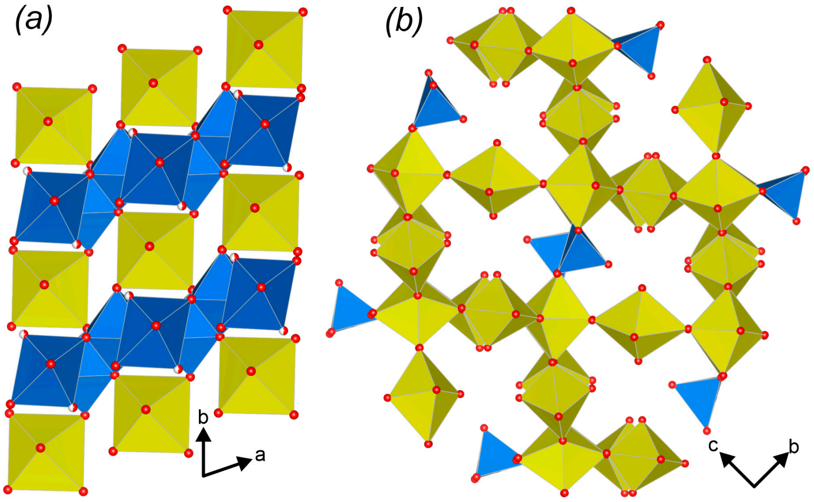

Figure 14. Framework architecture in the crystal structures of **76** (**a**), and **77** (**b**). Legend: see Figure 1.

The crystal structures based on 2D U-Mo complexes show less direct correlation. However, a few observations can be discussed. First, the better adaptability of the U-bearing substructural units to the changes of syntheses conditions should be mentioned. Thus, the cc2–1:2–4 topological type is found in the structures of ten compounds obtained over a wide temperature range: from room temperature, for **32**, to 700 °C, in case of compound **30**. It is of interest that both compounds crystallize in the same space group. It is also of interest that uranyl molybdate layers of the cc2–1:2–4 topology possess various symmetries. Moreover, for those structures where the minimum complexity of the layer is realized, the symmetry turns out to be higher (**26–27**, **29**), and vice versa; in structures where the structural complexity of the U-bearing layer is higher, a decrease in symmetry to monoclinic (**33**) and even triclinic (**28** and **31**) is observed (Figure 15e,f).

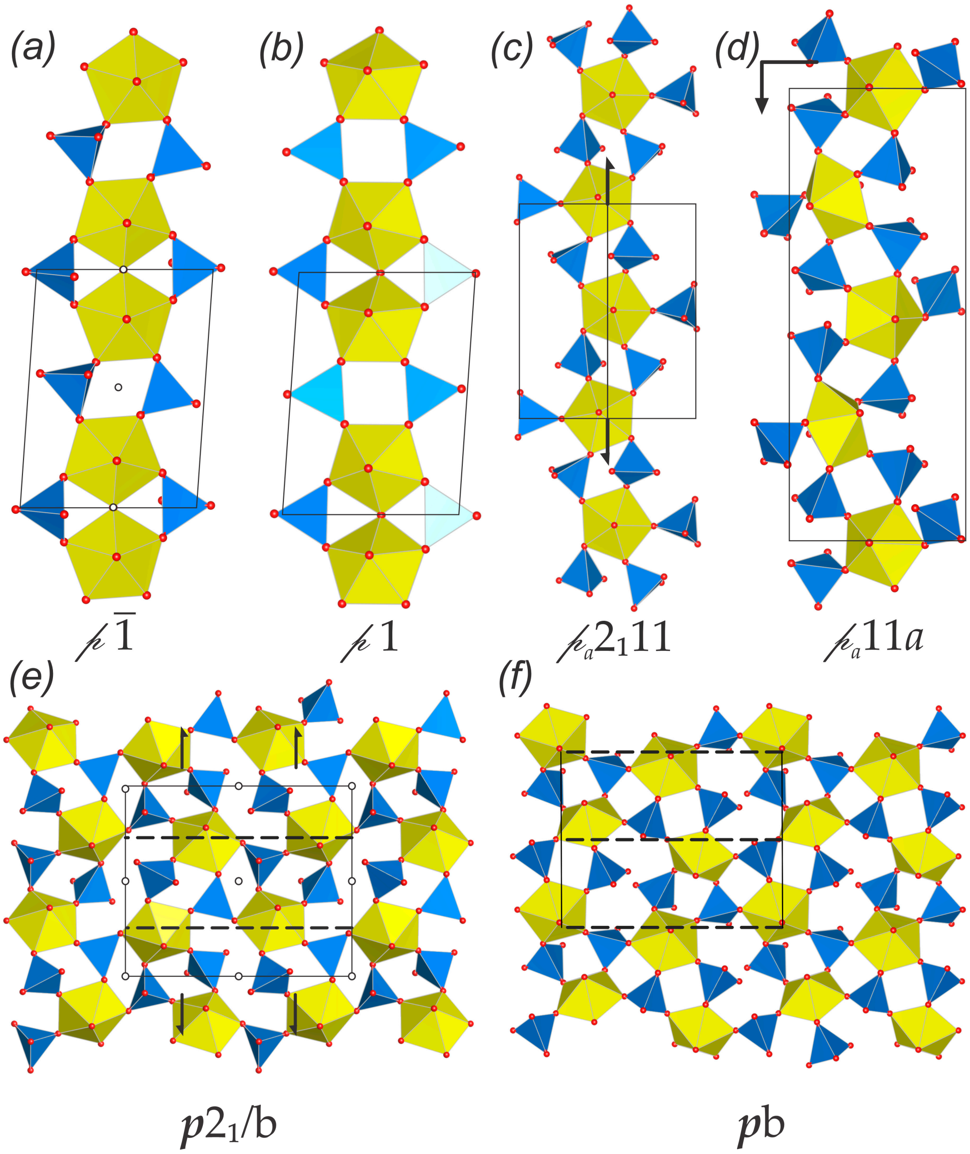

Figure 15. Uranyl molybdate complexes and their real (structural) rod and layer symmetry groups [26,27,29] in the structures of **18**,**19** (**a**), **20** (**b**), **22** (**c**), **23** (**d**), **26**–**27**,**29** €, and **33** (**f**); the structural symmetry of layers in **28** and **31** is *p*-1 with an arrangement of inversion centers as € (**e**). Legend: see Figure 1.

The structure of **35**, which is also based on layers of the cc2–1:2–4 type, has an anhydrous isomer analogue **37**, the structure of which is based on layers of the significantly rarer cc2–1:2–17 topology. Despite the differences in the topology and formation conditions of these compounds, the structural complexity parameters of their uranyl molybdate complexes are identical. Compound **35** has a very close composition with compound **69**, which is also obtained during hydrothermal synthesis and differs in hydration state. The latter is based on a framework formed by distorted layers of the cc2–1:2–4 topology (Figure 8). The significant difference in heating duration (2 and 72 h for **35** and **69**, respectively [60,91]) can be regarded as a possible factor that governs the aforementioned varieties.

Compound **38**, obtained by high-temperature solid-state synthesis, has a U-Se analogue, which has the same topology (cc2–2:3–14) of layered complexes and was obtained at room temperature [102].

The crystal structures of compounds **58–60** are based on frameworks constructed by layers of the cc2–2:3–14 topological type. These compounds were synthesized by heating with temperatures ranging from 180 to 700 °C, which demonstrates the great stability of the current 3D architecture.

Compound **68**, obtained as a result of high-pressure and high-temperature synthesis, is isotypic to compounds **64–67**, which were synthesized at significantly lower temperatures and pressures. It is of interest that this group of structures is based on a framework with a vertex-sharing interpolyhedral linkage, which was detected only at low temperature conditions in the case of uranyl sulfates [101].

In contrast, two other compounds, **76** and **78**, were obtained by high-pressure and high-temperature synthesis. Their structures are based on frameworks with dense manner of interpolyhedral linkage (Figures 11 and 14a).

Despite the considerable number of available compounds, it was impossible to correlate crystal chemical features and structural complexity parameters depending on the counter-ion, as was recently conducted for uranyl sulfates [101]; this is most likely due to the small number of structures known per particular topological type.

4. Conclusions

Summarizing the results of the review, a specific crystal chemistry of natural and synthetic uranyl molybdates attracts attention. First, one can note a significant discrepancy in the topological types for natural and synthetic phases, which is most likely due to elevated temperatures of laboratory experiments (up to 1000 °C), while natural phases apparently grow at significantly lower temperatures. At the same time, the prevalence of dense topologies (with edge-sharing interpolyhedral linkage) among natural phases can be noted, which is fully consistent with other recently considered mineral groups [26,27,29]. Uranyl molybdates demonstrate many similarities with compounds of other U-bearing groups; however, even topological matches do not lead to the appearance of completely isotypic compounds. It was recently shown that even if the structural architecture is preserved, a strikingly different manifestation of chemical and physical properties can be expected for molybdates [103].

As suggested in recent reviews [26–29], structural complexity parameters of uranyl molybdate compounds were calculated according to the “ladders of information” procedure [104], which allows us to distinguish the substructural units that play the most significant role, and which has the most impact on symmetry reduction or preservation. Structural complexity calculations confirm, in general, crystal chemical observations. Considering the prevalence of dense structures in which coordination polyhedra of uranium and molybdenum are connected through common edges, as well as framework architectures, one can expect a less significant influence of interlayer species on the formation of the crystal structure than the main U-bearing complexes. This is confirmed by clear dependencies shown on the graphs (Figure 16). The greater the structural complexity of the uranyl molybdate units, the more complex the entire crystal structure is. A slightly worse dependence for vertex-sharing layered structures is due to the lack of completeness and the diversity of available data. In addition, there is a tendency for complexity to increase with increasing density of the complex; the simplest structures are vertex-shared, while the complexity increases with the appearance of common edges.

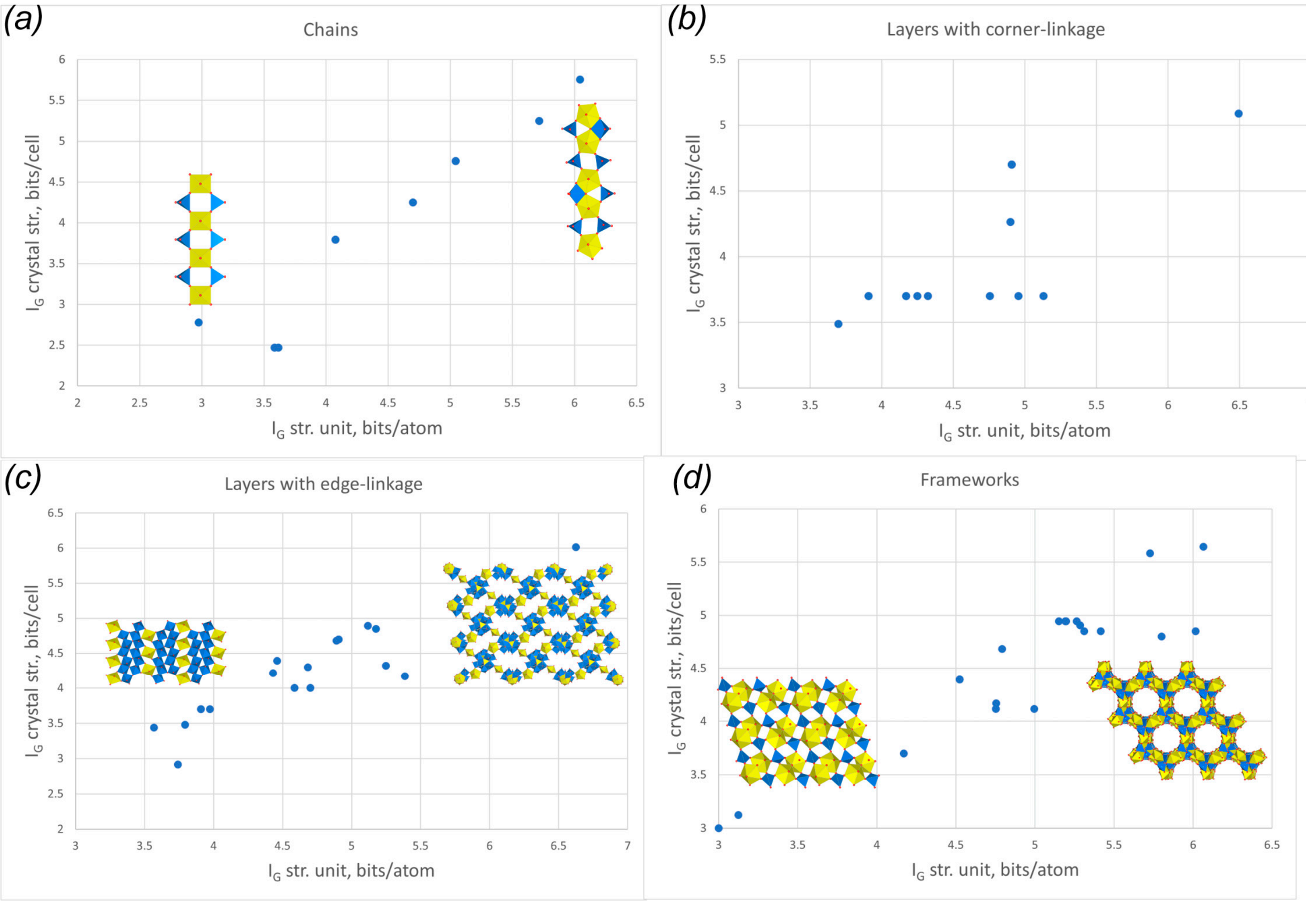

Figure 16. Correlation graphs of the entire structure complexity parameters with that for U-bearing structural unit for the structures based on U-Mo chains (**a**), layers with corner- (**b**) and edge-sharing linkage (**c**), frameworks (**d**).

Author Contributions: All authors (I.V.K., S.A.K. and V.V.G.) contributed equally to the Conceptualization; Methodology; Investigation; Writing-Original Draft Preparation; Writing-Review, and Editing; and Visualization. All authors have read and agreed to the published version of the manuscript.

Funding: This work was supported by the Russian Science Foundation (grant No. 23-17-00080).

Data Availability Statement: Data are contained within the paper.

Acknowledgments: An access to structural databases was provided by the X-ray Diffraction Centre of St. Petersburg State University.

Conflicts of Interest: The authors declare no conflicts of interest.

References

1. Basiev, T.T.; Sobol, A.A.; Voronko, Y.K.; Zverev, P.G. Spontaneous Raman Spectroscopy of Tungstate and Molybdate Crystals for Raman Lasers. *Opt. Mater.* **2000**, *15*, 205–216. [CrossRef]
2. Dorzhieva, S.G.; Sofich, D.O.; Bazarov, B.G.; Shendrik, R.Y.; Bazarova, J.G. Optical Properties of Molybdates Containing a Combination of Rare-Earth Elements. *Inorg. Mater.* **2021**, *57*, 54–59. [CrossRef]
3. Malavasi, L.; Fisher, C.A.J.; Islam, M.S. Oxide-ion and proton conducting electrolyte materials for clean energy applications: Structural and mechanistic features. *Chem. Soc. Rev.* **2010**, *39*, 4370–4387. [CrossRef] [PubMed]
4. Lind, C.; VanDerveer, D.G.; Wilkinson, A.P.; Chen, J.H.; Vaughan, M.T.; Weidner, D.J. New high-pressure form of the negative thermal expansion materials zirconium molybdate and hafnium molybdate. *Chem. Mater.* **2001**, *13*, 487–490. [CrossRef]
5. Murphy, G.L.; Kegler, P.; Klinkenberg, M.; Wang, S.; Alekseev, E.V. Extreme condition high temperature and high pressure studies of the K–U–Mo–O system. *Dalton Trans.* **2020**, *49*, 15843–15853. [CrossRef] [PubMed]

6. Finch, R.J.; Murakami, T. Systematics and Paragenesis of Uranium Minerals. In *Uranium: Mineralogy, Geochemistry and the Environment*; Burns, P.C., Finch, R.J., Eds.; Reviews in Mineralogy; Mineralogical Society of America: Chantilly, VA, USA, 1999; Volume 38, pp. 91–180.
7. Krivovichev, S.V.; Burns, P.C. Crystal chemistry of uranyl molybdates. III. New structural themes in $Na_6[(UO_2)_2O(MoO_4)_4]$, $Na_6[(UO_2)(MoO_4)_4]$ and $K_6[(UO_2)_2O(MoO_4)_4]$. *Can. Mineral.* **2001**, *39*, 197–206. [CrossRef]
8. Buck, E.C.; Wronkiewicz, D.J.; Finn, P.A.; Bates, J.K. A new uranyl oxide hydrate phase derived from spent fuel alteration. *J. Nucl. Mater.* **1997**, *249*, 70–76. [CrossRef]
9. Buck, E.C.; Wronkiewicz, D.J. Uranium Mineralogy and the Geologic Disposal of Spent Nuclear Fuel. *Rev. Mineral. Geochem.* **1999**, *38*, 474–497.
10. Lafuente, B.; Downs, R.T.; Yang, H.; Stone, N. The power of databases: The RRUFF project. In *Highlights in Mineralogical Crystallography*; Armbruster, T., Danisi, R.M., Eds.; De Gruyter: Berlin, Germany, 2015; pp. 1–30.
11. Burns, P.C.; Miller, M.L.; Ewing, R.C. U^{6+} minerals and inorganic phases: A comparison and hierarchy of structures. *Can. Mineral.* **1996**, *34*, 845–880.
12. Lussier, A.J.; Lopez, R.A.K.; Burns, P.C. A revised and expanded structure hierarchy of natural and synthetic hexavalent uranium compounds. *Can. Mineral.* **2016**, *54*, 177–283. [CrossRef]
13. Hawthorne, F.C. Graphical enumeration of polyhedral clusters. *Acta Crystallogr. A* **1983**, *39*, 724–736. [CrossRef]
14. Krivovichev, S.V. Combinatorial topology of salts of inorganic oxoacids: Zero-, one- and two-dimensional units with corner-sharing between coordination polyhedra. *Crystallogr. Rev.* **2004**, *10*, 185–232. [CrossRef]
15. Krivovichev, S.V. *Structural Crystallography of Inorganic Oxysalts*; Oxford University Press: Oxford, UK, 2008; p. 303.
16. Krivovichev, S.V. Topological complexity of crystal structures: Quantitative approach. *Acta Crystallogr. A* **2012**, *68*, 393–398. [CrossRef] [PubMed]
17. Krivovichev, S.V. Structural complexity of minerals: Information storage and processing in the mineral world. *Mineral. Mag.* **2013**, *77*, 275–326. [CrossRef]
18. Krivovichev, S.V. Which inorganic structures are the most complex? *Angew. Chem. Int. Ed.* **2014**, *53*, 654–661. [CrossRef] [PubMed]
19. Krivovichev, S.V. Structural complexity of minerals and mineral parageneses: Information and its evolution in the mineral world. In *Highlights in Mineralogical Crystallography*; Danisi, R., Armbruster, T., Eds.; Walter de Gruyter: Berlin, Germany, 2015; pp. 31–73.
20. Krivovichev, S.V. Structural complexity and configurational entropy of crystalline solids. *Acta Crystallogr. B* **2016**, *72*, 274–276. [CrossRef] [PubMed]
21. Gurzhiy, V.V.; Tyumentseva, O.S.; Izatulina, A.R.; Krivovichev, S.V.; Tananaev, I.G. Chemically Induced Polytypic Phase Transitions in the $Mg[(UO_2)(TO_4)_2(H_2O)](H_2O)_4$ (T = S, Se) System. *Inorg. Chem.* **2019**, *58*, 14760–14768. [CrossRef] [PubMed]
22. Gurzhiy, V.V.; Tyumentseva, O.S.; Belova, E.V.; Krivovichev, S.V. Chemically induced symmetry breaking in the crystal structure of guanidinium uranyl sulfate. *Mendeleev Commun.* **2019**, *29*, 408–410. [CrossRef]
23. Tyumentseva, O.S.; Kornyakov, I.V.; Britvin, S.N.; Zolotarev, A.A.; Gurzhiy, V.V. Crystallographic Insights into Uranyl Sulfate Minerals Formation: Synthesis and Crystal Structures of Three Novel Cesium Uranyl Sulfates. *Crystals* **2019**, *9*, 660. [CrossRef]
24. Kornyakov, I.V.; Kalashnikova, S.A.; Gurzhiy, V.V.; Britvin, S.N.; Belova, E.V.; Krivovichev, S.V. Synthesis, characterization and morphotropic transitions in a family of $M[(UO_2)(CH_3COO)_3](H_2O)_n$ (M = Na, K, Rb, Cs; n = 0–1.0) compounds. *Z. Kristallogr.* **2020**, *235*, 95–103. [CrossRef]
25. Kornyakov, I.V.; Tyumentseva, O.S.; Krivovichev, S.V.; Gurzhiy, V.V. Dimensional evolution in hydrated K+-bearing uranyl sulfates: From 2D-sheets to 3D frameworks. *Cryst. Eng. Comm.* **2020**, *22*, 4621–4629. [CrossRef]
26. Gurzhiy, V.V.; Plasil, J. Structural complexity of natural uranyl sulfates. *Acta Crystallogr. B* **2019**, *75*, 39–48. [CrossRef] [PubMed]
27. Gurzhiy, V.V.; Kuporev, I.V.; Kovrugin, V.M.; Murashko, M.N.; Kasatkin, A.V.; Plášil, J. Crystal chemistry and structural complexity of natural and synthetic uranyl selenites. *Crystals* **2019**, *9*, 639. [CrossRef]
28. Krivovichev, V.G.; Krivovichev, S.V.; Charykova, M.V. Selenium Minerals: Structural and Chemical Diversity and Complexity. *Minerals* **2019**, *9*, 455. [CrossRef]
29. Gurzhiy, V.V.; Kalashnikova, S.A.; Kuporev, I.V.; Plášil, J. Crystal Chemistry and Structural Complexity of the Uranyl Carbonate Minerals and Synthetic Compounds. *Crystals* **2021**, *11*, 704. [CrossRef]
30. Blatov, V.A.; Shevchenko, A.P.; Proserpio, D.M. Applied topological analysis of crystal structures with the program package ToposPro. *Cryst. Growth. Des.* **2014**, *14*, 3576–3586. [CrossRef]
31. Sarp, H.; Chiappero, P.J. Deloryite, $Cu_4(UO_2)(MoO_4)_2(OH)_6$, a new mineral from the Cap Garonne mine near Le Pradet, Var, France. *Neues Jahrb. Mineral. Monatshefte* **1992**, *2*, 58–64.
32. Tali, R.; Tabachenko, V.V.; Kovba, L.M. Crystal structure of $Cu_4UO_2(MoO_4)_2(OH)_6$. *Russ. J. Inorg. Chem.* **1993**, *38*, 1350–1352.
33. Pushcharovsky, D.Y.; Rastsvetaeva, R.K.; Sarp, H. Crystal structure of deloryite, $Cu_4(UO_2)[Mo_2O_8](OH)_6$. *J. Alloys Compd.* **1996**, *239*, 23–26. [CrossRef]
34. Brophy, G.P.; Kerr, P.F. *Hydrous Uranium Molybdate in Maryvale Ore*; Annual Report for June 30, 1952 to April 1, 1953 RME-3046; U.S. Atomic Energy Commission: Oak Ridge, Tennessee, 1953; pp. 45–51.
35. Coleman, R.G.; Appleman, D.E. Umohoite from the Lucky MC mine, Wyoming. *Am. Mineral.* **1957**, *42*, 657–660.
36. Skvortsova, K.V.; Kopchenova, E.V.; Silant'eva, N.I.; Sidorenko, G.A.; Dara, A.D. On the conditions of umohoite formation on U.S.S.R. uranium-molybdenum deposits. *Geol. Ore Depos.* **1961**, *5*, 53–63.

37. Krivovichev, S.V.; Burns, P.C. Crystal chemistry of uranyl molybdates. I. The structure and formula of umohoite. *Can. Mineral.* **2000**, *38*, 717–726. [CrossRef]
38. Sidorenko, G.A.; Rastsvetaeva, R.K.; Chukanov, N.V.; Chistyakova, N.I.; Barinova, A.V. Umohoite: New data on its mineralogy and crystal-chemistry. *Zap. Vseross. Mineral. Obs.* **2003**, *132*, 73–80.
39. Rastsvetaeva, R.K.; Barinova, A.V.; Sidorenko, G.A.; Pushcharovskii, D.Y. Crystal structure of triclinic umohoite $[UMoO_6(H_2O)](H_2O)$. *Dokl. Akad. Nauk* **2000**, *373*, 202–205.
40. Makarov, E.S.; Anikina, L.I. Crystal structure of umohoite $(UMoO_6(H_2O)_2){\cdot}2H_2O$. *Geochemistry* **1963**, *1*, 14–21.
41. Soboleva, M.V.; Pudovkina, I.A. Iriginite. In *Uranium Minerals Handbook*; Gosgeoltekhizdat: Moscow, Russia, 1957; pp. 249–251. (In Russian)
42. Epshtein, G.Y. On the molybdates of uranium—Moluranite and iriginite. *Zap. Vsesoyuznogo Mineral. Obs.* **1959**, *88*, 564–570. (In Russian)
43. Serezhkin, V.N.; Chuvaev, V.F.; Kovba, L.M.; Trunov, V.K. The structure of synthetic iriginite. *Dokl. Akad. Nauk SSSR* **1973**, *210*, 873–876. (In Russian)
44. Krivovichev, S.V.; Burns, P.C. The crystal chemistry of uranyl molybdates. II. The crystal structure of iriginite. *Can. Mineral.* **2000**, *38*, 847–851. [CrossRef]
45. Elliott, P.; Plášil, J.; Petříček, V.; Čejka, J.; Bindi, L. Twinning and incomensurate modulation in baumoite, $Ba_{0.5}[(UO_2)_3O_8Mo_2(OH)_3](H_2O)_{\sim 3}$, the first natural Ba uranyl molybdate. *Mineral. Mag.* **2019**, *83*, 507–514. [CrossRef]
46. Chen, Z.; Luo, K.; Tan, F.; Zhang, Y.; Gu, X. Tengchongite, a new mineral of hydrated calcium uranyl molybdate. *Kexue Tongbao* **1986**, *31*, 396–401.
47. Li, T.; Fan, G.; Ge, X.; Wang, T.; Yu, A.; Deng, L. Crystal structure of tengchongite with a revised chemical formula $Ca(UO_2)_6(MoO_4OH)_2O_2(OH)_4{\cdot}9H_2O$. *Can. Mineral.* **2022**, *60*, 533–542. [CrossRef]
48. Soboleva, M.V.; Pudovkina, I.A. Moluranite. In *Uranium Minerals Handbook*; Gosgeoltekhizdat: Moscow, Russia, 1957; pp. 252–253.
49. Kopchenova, E.V.; Skvortsova, K.V.; Silantieva, N.I.; Sidorenko, G.A.; Mikhailova, L.V. Mourite, a new supergene uranium-molybdenum mineral. *Zap. Vsesoyuznogo Mineral. Obs.* **1962**, *91*, 67–71.
50. Smith, M.L.; Marinenko, J.; Weeks, A.D. Comparison of mourite from Karnes County, Texas with mourite from the U.S.S.R. *Am. Mineral.* **1971**, *56*, 163–173.
51. Rudnitskaya, L.S. Calcium molybdate of uranium. *Yad. Goryuchee I Reakt. Met.* **1959**, *3*, 160–161.
52. Fedorov, O.V. The second finding of the calcium molybdate of uranium in the USSR. *Zap. Vsesoyuznogo Mineral. Obs.* **1963**, *92*, 464–465.
53. Sidorenko, G.A.; Chistyakova, N.I.; Chukanov, N.V.; Naumova, I.S.; Rassulov, V.A. Carcurmolite: New data on chemical composition and constitution the mineral. *New Data Miner.* **2005**, *40*, 29–36.
54. Frost, R.L.; Čejka, J.; Dickfos, M.J. Raman and infrared spectroscopic study of the molybdate-containing uranyl mineral calcurmolite. *J. Raman Spectrosc.* **2008**, *39*, 779–785. [CrossRef]
55. Vaes, J.F. Cousiniet, een nieuw uraanmineraal. *Geol. Mijnb.* **1958**, *20*, 449.
56. Deliens, M. Une association de molybdates d'uranium de Shinkolobwe (Région du Shaba, République du Zaire). *Ann. Soc. Géol. Belg.* **1975**, *98*, 155–160.
57. Skvortsova, K.V.; Sidorenko, G.A. Sedovite, a new supergene mineral of uranium and molybdenum. *Zap. Vsesoyuznogo Mineral. Obs.* **1965**, *94*, 548–554.
58. Krivovichev, S.V.; Burns, P.C. Crystal chemistry of uranyl molybdates. VI. New uranyl molybdate units in the structures of $Cs_4[(UO_2)_3O(MoO_4)_2(MoO_5)]$ and $Cs_6[(UO_2)(MoO_4)_4]$. *Can. Mineral.* **2002**, *40*, 201–209. [CrossRef]
59. Krivovichev, S.V.; Burns, P.C. Crystal Chemistry of Rubidium Uranyl Molybdates: Crystal Structures of $Rb_6[(UO_2)(MoO_4)_4]$, $Rb_6[(UO_2)_2O(MoO_4)_4]$, $Rb_2[(UO_2)(MoO_4)_2]$, $Rb_2[(UO_2)_2(MoO_4)_3]$ and $Rb_2[(UO_2)_6(MoO_4)_7(H_2O)_2$. *J. Solid State Chem.* **2002**, *168*, 245–258. [CrossRef]
60. Krivovichev, S.V.; Burns, P.C. Crystal chemistry of uranyl molybdates. VIII. Crystal structures of $Na_3Tl_3[(UO_2)(MoO_4)_4]$, $Na_{13-x}Tl_{3+x}[(UO_2)(MoO_4)_3]_4(H_2O)_{6+x}$ (x = 0.1), $Na_3Tl_5[(UO_2)(MoO_4)_3]_2(H_2O)_3$ and $Na_2[(UO_2)(MoO_4)_2](H_2O)_4$. *Can. Mineral.* **2003**, *41*, 707–719. [CrossRef]
61. Alekseev, E.V.; Krivovichev, S.V.; Armbruster, T.; Depmeier, W.; Suleimanov, E.V.; Chuprunov, E.V.; Golubeva, A.V. Dimensional reduction in alkali metal uranyl molybdates: Synthesis and structure of $Cs_2[(UO_2)O(MoO_4)]$. *Z. Anorg. Allg. Chem.* **2007**, *633*, 1979–1984. [CrossRef]
62. Krivovichev, S.V.; Burns, P.C. Synthesis and crystal structure of $Li_2[(UO_2)(MoO_4)_2]$, a uranyl molybdate with chains of corner-sharing uranyl square bipyramids and MoO_4 tetrahedra. *Solid State Sci.* **2003**, *5*, 481–485. [CrossRef]
63. Yagoubi, S.; Obbade, S.; Saad, S.; Abraham, F. From ${}_\infty{}^1[(UO_2)_2O(MoO_4)_4]^{6-}$ to ${}_\infty{}^1[(UO_2)_2(MoO_4)_3(MoO_5)]^{6-}$ infinite chains in $A_6U_2Mo_4O_{21}$ (A = Na, K, Rb, Cs) compounds: Synthesis and crystal structure of $Cs_6[(UO_2)_2(MoO_4)_3(MoO_5)]$. *J. Solid State Chem.* **2011**, *184*, 971–981. [CrossRef]
64. Sykora, R.E.; McDaniel, S.M.; Wells, D.M.; Albrecht-Schmitt, T.E. Mixed-Metal Uranium(VI) Iodates: Hydrothermal Syntheses, Structures, and Reactivity of $Rb[UO_2(CrO_4)(IO_3)(H_2O)]$, $A_2[UO_2(CrO_4)(IO_3)_2]$ (A = K, Rb, Cs), and $K_2[UO_2(MoO_4)(IO_3)_2$. *Inorg. Chem.* **2002**, *41*, 5126–5132. [CrossRef] [PubMed]
65. Krivovichev, S.V.; Burns, P.C. Crystal chemistry of uranyl molybdates. XI. Crystal structures of $Cs_2[(UO_2)(MoO_4)_2]$ and $Cs_2[(UO_2)(MoO_4)_2](H_2O)$. *Can. Mineral.* **2005**, *43*, 713–720. [CrossRef]

66. Rastsvetaeva, R.K.; Barinova, A.V.; Fedoseev, A.M.; Budantseva, N.A. Synthesis and crystal structure of a new hydrated cesium uranyl molybdate $Cs_2UO_2(MoO_4)_2(H_2O)$. *Dokl. Akad. Nauk* **1999**, *365*, 68–71. (In Russian)
67. Sadikov, G.G.; Krasovskaya, T.I.; Polyakov, Y.A.; Nikolaev, V.P. Structure and spectral analysis of potassium uranyl dimolybdate. *Izv. Akad. Nauk SSSR Neorg. Mater.* **1988**, *24*, 109–115. (In Russian)
68. Krivovichev, S.V.; Finch, R.J.; Burns, P.C. Crystal chemistry of uranyl molybdates. V. Topologically distinct uranyl dimolybdate sheets in the structures of $Na_2[(UO_2)(MoO_4)_2]$ and $K_2[(UO_2)(MoO_4)_2](H_2O)$. *Can. Mineral.* **2002**, *40*, 193–200. [CrossRef]
69. Krivovichev, S.V.; Burns, P.C. Combinatorial topology of uranyl molybdate sheets: Syntheses and crystal structures of $(C_6H_{14}N_2)_3[(UO_2)_5(MoO_4)_8](H_2O)_4$ and $(C_2H_{10}N_2)[(UO_2)(MoO_4)_2]$. *J. Solid State Chem.* **2003**, *170*, 106–117. [CrossRef]
70. Khrustalev, V.N.; Andreev, G.B.; Antipin, M.Y.; Fedoseev, A.M.; Budantseva, N.A.; Shirokova, I.B. Synthesis and crystal structure of rubidium uranyl dimolybdate $Rb_2UO_2(MoO_4)_2(H_2O)$. *Zhurnal Neorg. Khimii* **2000**, *45*, 1996–1998. (In Russian)
71. Krivovichev, S.V.; Locock, A.J.; Burns, P.C. Lone electron pair stereoactivity, cation arrangements and distortion of heteropolyhedral sheets in the structures of $Tl_2[(UO_2)(AO_4)_2]$ (A = Cr, Mo). *Z. Kristallogr.* **2005**, *220*, 10–18. [CrossRef]
72. Shiv Halasyamani, P.; Francis, R.J.; Walker, S.M.; O'Hare, D. New Layered Uranium(VI) Molybdates: Syntheses and Structures of $(NH_3(CH_2)_3NH_3)(H_3O)_2(UO_2)_3(MoO_4)_5$, $C(NH_2)_3(UO_2)(OH)(MoO_4)$, $(C_4H_{12}N_2)(UO_2)(MoO_4)_2$, and $(C_5H_{14}N_2)(UO_2)(MoO_4)_2(H_2O)$. *Inorg. Chem.* **1999**, *38*, 271–279. [CrossRef]
73. Krivovichev, S.V.; Cahill, C.L.; Burns, P.C. Syntheses and Crystal Structures of Two Topologically Related Modifications of $Cs_2[(UO_2)_2(MoO_4)_3]$. *Inorg. Chem.* **2002**, *41*, 34–39. [CrossRef]
74. Nazarchuk, E.V.; Charkin, D.; Siidra, O.; Kalmykov, S. Organically Templated Layered Uranyl Molybdate $[C_3H_9NH^+]_4[(UO_2)_3(MoO_4)_5]$ Structurally Based on Mineral-Related Modular Units. *Minerals* **2020**, *10*, 659. [CrossRef]
75. Lee, M.R.; Jaulmes, S. Nouvelle serie d'oxydes derives de la structure de α-U_3U_8: $M^{ii}UMo_4O_{16}$. *J. Solid State Chem.* **1987**, *67*, 364–368. [CrossRef]
76. Krivovichev, S.V.; Burns, P.C. Crystal chemistry of uranyl molybdates. VII. An iriginite-type sheet of polyhedra in the structure of $[(UO_2)Mo_2O_7(H_2O)_2]$. *Can. Mineral.* **2002**, *40*, 1571–1577. [CrossRef]
77. Krivovichev, S.V.; Burns, P.C. Synthesis and Structure of $Ag_6[(UO_2)_3O(MoO_4)_5]$: A Novel Sheet of Triuranyl Clusters and MoO_4 Tetrahedra. *Inorg. Chem.* **2002**, *41*, 4108–4110. [CrossRef]
78. Kotvanova, M.K.; Molchanov, V.N.; Torchenkova, E.A.; Spitsyn, V.I. The crystal structure of $(NH_4)_4[(UO_2)_2(H_2O)_3UMo_{12}O_{42})(H_2O)_{18}$. *Zhurnal Neorg. Khimii* **1984**, *29*, 1790–1797. (In Russian)
79. Nazarchuk, E.V.; Siidra, O.I.; Krivovichev, S.V.; Malcherek, T.; Depmeier, W. First Mixed Alkaline Uranyl Molybdates: Synthesis and Crystal Structures of $CsNa_3[(UO_2)_4O_4(Mo_2O_8)]$ and $Cs_2Na_8[(UO_2)_8O_8(Mo_5O_{20})]$. *Z. Anorg. Allg. Chem.* **2009**, *635*, 1231–1235. [CrossRef]
80. Krivovichev, S.V.; Burns, P.C. Crystal chemistry of uranyl molybdates. X. The crystal structure of $Ag_{10}[(UO_2)_8O_8(Mo_5O_{20})]$. *Can. Mineral.* **2003**, *41*, 1455–1462. [CrossRef]
81. Krivovichev, S.V. $K_2Na_8(UO_2)_8Mo_4O_{24}[(S,Mo)O_4]$, the first uranium molybdosulfate: Synthesis, crystal structure, and comparison to related compounds. *J. Geosci.* **2014**, *59*, 115–121. [CrossRef]
82. Alekseev, E.V.; Suleimanov, E.V.; Chuprunov, E.V.; Golubev, A.V.; Fukin, G.K.; Marychev, M.O. Synthesis and Crystal Structure of a New Representative of the $Rb_2U_2MoO_{10}$ Uranomolybdate Series. *Russ. J. Inorg. Chem.* **2007**, *52*, 1446–1449. [CrossRef]
83. Obbade, S.; Yagoubi, S.; Dion, C.; Saadi, M.; Abraham, F. Synthesis, crystal structure and electrical characterization of two new potassium uranyl molybdates $K_2(UO_2)_2(MoO_4)O_2$ and $K_8(UO_2)_8(MoO_5)_3O_6$. *J. Solid State Chem.* **2003**, *174*, 19–31. [CrossRef]
84. Krivovichev, S.V.; Burns, P.C. Crystal chemistry of uranyl molybdates. IX. A novel uranyl molybdate sheet in the structure of $Tl_2[(UO_2)_2O(MoO_5)]$. *Can. Mineral.* **2003**, *41*, 1225–1231. [CrossRef]
85. Nazarchuk, E.V.; Krivovichev, S.V.; Burns, P.C. Crystal structure and phase transformations of $Ca[(UO_2)_6(MoO_4)_7(H_2O)_2](H_2O)_n$ (n~7.6). *Zap. Ross. Mineral.* **2005**, *134*, 110–117. (In Russian)
86. Nazarchuk, E.V.; Krivovichev, S.V.; Burns, P.C. Crystal structure of $Tl_2[(UO_2)_2(MoO_4)_3]$ and crystal chemistry of the compounds $M2[(UO_2)_2(MoO_4)_3]$ (M = Tl, Rb, Cs). *Radiokhimiya* **2005**, *47*, 408–411. [CrossRef]
87. Serezhkin, V.N.; Efremov, V.A.; Trunov, V.K. The crystal structure of alpha-$UO_2MoO_4(H_2O)_2$. *Kristallografiya* **1980**, *25*, 861–865. (In Russian)
88. Tabachenko, V.V.; Kovba, L.M.; Serezhkin, V.N. Crystal structures of $Mg(UO_2)_6(MoO_4)_7(H_2O)_{18}$ and $Sr(UO_2)_6(MoO_4)_7(H_2O)_{15}$. *Koord. Khimiya* **1984**, *10*, 558–562. (In Russian)
89. Krivovichev, S.V.; Burns, P.C. Crystal chemistry of uranyl molybdates. IV. The structures of $M_2[(UO_2)_6(MoO_4)_7(H_2O)_2]$ (M = Cs, NH_4). *Can. Mineral.* **2001**, *39*, 207–214. [CrossRef]
90. Nazarchuk, E.V.; Siidra, O.I.; Krivovichev, S.V. Synthesis and Crystal Structure of $Ag_2[(UO_2)_6(MoO_4)_7(H_2O)_2](H_2O)_2$. *Radiochemistry* **2016**, *58*, 1–5. [CrossRef]
91. Wang, Y.; Wang, Y.; Dai, X.; Liu, W.; Yin, X.; Chen, L.; Zhai, F.; Diwu, J.; Zhang, C.; Zhou, R.; et al. Inorganic X-ray scintillators based on a previously unnoticed but intrinsically advantageous metal center. *Inorg. Chem.* **2019**, *58*, 2807–2812. [CrossRef] [PubMed]
92. Tabachenko, V.V.; Balashov, V.L.; Kovba, L.M.; Serezhkin, V.N. Crystal Structure of Barium Uranyl Molybdate $Ba(UO_2)_3(MoO_4)_4(H_2O)_4$. *Koord. Khimiya* **1984**, *10*, 854–857. (In Russian)
93. Tabachenko, V.V.; Kovba, L.M.; Serezhkin, V.N. The crystal structure of molybdatouranylates of magnesium and zinc of composition $M(UO_2)_3(MoO_4)_4(H_2O)_8$ (M = Mg, Zn). *Koord. Khimiya* **1983**, *9*, 1568–1571. (In Russian)

94. Krivovichev, S.V.; Cahill, C.L.; Burns, P.C. A novel open framework uranyl molybdate: Synthesis and structure of $(NH_4)_4((UO_2)_5(MoO_4)_7)(H_2O)_5$. *Inorg. Chem.* **2003**, *42*, 2459–2464. [CrossRef]
95. Krivovichev, S.V.; Cahill, C.L.; Nazarchuk, E.V.; Burns, P.C.; Armbruster, T.; Depmeier, W. Chiral open-framework uranyl molybdates. 1. Topological diversity: Synthesis and crystal structure of $[(C_2H_5)_2NH_2]_2[(UO_2)_4(MoO_4)_5(H_2O)](H_2O)$. *Microporous Mesoporous Mater.* **2005**, *78*, 209–215. [CrossRef]
96. Serezhkin, V.N.; Trunov, V.K.; Makarevich, L.G. The refined crystal structure of uranyl molybdate. *Kristallografiya* **1980**, *25*, 858–860.
97. Alekseev, E.V.; Krivovichev, S.V.; Malcherek, T.; Depmeier, W. One-dimensional array of two- and three-center cation–cation bonds in the structure of $Li_4[(UO_2)_{10}O_{10}(Mo_2O_8)]$. *Inorg. Chem.* **2007**, *46*, 8442–8444. [CrossRef]
98. Smith, D.K. Uranium mineralogy. In *Uranium Geochemistry, Mineralogy, Geology, Exploration and Resources*; De Vivo, B., Ippolito, F., Capaldi, G., Simpson, P.R., Eds.; Institute of Mining and Metallurgy: London, UK, 1984; pp. 43–88.
99. Gaines, R.V.; Skinner, H.C.W.; Foord, E.E.; Mason, B.; Rosenzweig, A. *Dana's New Mineralogy*, 8th ed.; John Wiley & Sons: New York, NY, USA, 1997.
100. Obbade, S.; Dion, C.; Bekaert, E.; Yagoubi, S.; Saadi, M.; Abraham, F. Synthesis and crystal structure of new uranyl tungstates $M_2(UO_2)(W_2O_8)$ (M=Na, K), $M_2(UO_2)_2(WO_5)O$ (M=K, Rb), and $Na_{10}(UO2)8(W5O_{20})O_8$. *J. Solid State Chem.* **2003**, *172*, 305–318. [CrossRef]
101. Durova, E.V.; Kuporev, I.V.; Gurzhiy, V.V. Organically Templated Uranyl Sulfates and Selenates: Structural Complexity and Crystal Chemical Restrictions for Isotypic Compounds Formation. *Int. J. Mol. Sci.* **2023**, *24*, 13020. [CrossRef] [PubMed]
102. Kovrugin, V.M.; Gurzhiy, V.V.; Krivovichev, S.V. Structural topology and dimensional reduction in uranyl oxysalts: Eight novel phases in the methylamine–$(UO_2)(NO_3)_2$–H_2SeO_4–H_2O system. *Struct. Chem.* **2012**, *23*, 2003–2017. [CrossRef]
103. Gurzhiy, V.V.; Kornyakov, I.V.; Szymanowski, J.E.S.; Felton, D.; Tyumentseva, O.S.; Krzhizhanovskaya, M.G.; Krivovichev, S.V.; Burns, P.C. Chemically-induced structural variations of a family of $Cs_2[(AnO_2)_2(TO_4)_3]$ (An = U, Np; T = S, Se, Cr, Mo) compounds: Thermal behavior, calorimetry studies and spectroscopy characterization of Cs uranyl sulfate and selenate. *J. Solid State Chem.* **2020**, *282*, 121077–121084. [CrossRef]
104. Krivovichev, S.V. Ladders of information: What contributes to the structural complexity in inorganic crystals. *Z. Kristallogr.* **2018**, *233*, 155–161. [CrossRef]